Robust circadian clocks from coupled protein modification and transcription-translation cycles

David Zwicker,[1] David K. Lubensky,[2] and Pieter Rein ten Wolde[1]

[1]*FOM Institute for Atomic and Molecular Physics (AMOLF),*
Science Park 104, 1098 XG Amsterdam, The Netherlands
[2]*Department of Physics, University of Michigan, Ann Arbor, MI 48109-1040*

The cyanobacterium *Synechococcus elongatus* uses both a protein phosphorylation cycle and a transcription-translation cycle to generate circadian rhythms that are highly robust against biochemical noise. We use stochastic simulations to analyze how these cycles interact to generate stable rhythms in growing, dividing cells. We find that a protein phosphorylation cycle by itself is robust when protein turnover is low. For high decay or dilution rates (and co mpensating synthesis rate), however, the phosphorylation-based oscillator loses its integrity. Circadian rhythms thus cannot be generated with a phosphorylation cycle alone when the growth rate, and consequently the rate of protein dilution, is high enough; in practice, a purely post-translational clock ceases to function well when the cell doubling time drops below the 24 hour clock period. At higher growth rates, a transcription-translation cycle becomes essential for generating robust circadian rhythms. Interestingly, while a transcription-translation cycle is necessary to sustain a phosphorylation cycle at high growth rates, a phosphorylation cycle can dramatically enhance the robustness of a transcription-translation cycle at lower protein decay or dilution rates. Our analysis thus predicts that both cycles are required to generate robust circadian rhythms over the full range of growth conditions.

I. INTRODUCTION

Many organisms use circadian clocks to anticipate changes between day and night [1]. It had long been believed that these clocks are driven primarily by transcription-translation cycles (TTCs) built on negative feedback. However, while some circadian clocks can maintain robust rhythms for years in the absence of any daily cue [1], recent experiments have vividly demonstrated that gene expression is often highly stochastic [2]. This raises the question of how these clocks can be robust against biochemical noise. In multicellular organisms, the robustness might be explained by intercellular interactions [3, 4], but it is now known that even unicellular organisms can have very stable circadian rhythms. The clock of the cyanbacterium *Synechococcus elongatus*, for example, has a correlation time of several months [9], even though the clocks of the different cells in a population hardly interact with one another [6, 9]. Interestingly, it has recently been discovered that the *S. elongatus* clock also includes a protein phosphorylation cycle (PPC) that can run independently of the TTC [7, 8]. It has been suggested that this protein modification oscillator [8], possibly in combination with the transcription-translation oscillator [15], is responsible for the clock's striking noise resistance. Here, we use mathematical modeling to study how these two clocks interact in growing, dividing cells. We find that the PPC alone is very stable when cell growth is negligible, but it begins to fail as the growth rate increases, and for doubling times typical of *S. elongatus* it cannot function without help from a TTC. We then use stochastic simulations to show that a PPC can, however, dramatically enhance the robustness of a TTC, especially when cells are growing slowly. The two mechanisms thus perform best in complemen-

tary situations, and it is likely that both oscillators are necessary to maintain even minimal clock stability across the full range of conditions and growth rates that bacteria encounter in the wild. Importantly, the TTC and the PPC in *S. elongatus* are much more tightly intertwined than conventional coupled phase oscillators; as a result, the combination of the two far outperforms not just each of its two components individually, but also a hypothetical system in which the two parts are coupled in normal textbook fashion [10].

In *S. elongatus*, the central components of the clock are the three genes *kaiA*, *kaiB*, and *kaiC* [11]. Under continuous light conditions, the levels of mRNA from the *kaiBC* operon and of the protein KaiC oscillate in a circadian fashion with a 6 hour lag between their peaks [12]. Overexpression of phosphorylated KaiC abolishes *kaiBC* expression [13, 14], while a transient increase in KaiC resets the phase of the oscillator [12]. These observations led to the proposal that the Kai system is a transcription-translation oscillator, with KaiC negatively regulating its own transcription. In 2005, however, Kondo and coworkers showed that KaiC is phosphorylated in a cyclical manner with a period of 24 hours, even when *kaiBC* transcription is inhibited [7]. Still more remarkably, the rhythmic phosphorylation of KaiC could be reconstituted in the test tube in the presence of only KaiA, KaiB, and ATP [8]. This raised the possibility that the principal pacemaker of the clock is not a transcription-translation cycle, but a protein phosphorylation cycle [8]. Yet, in 2008, the same group showed that circadian oscillations of gene expression persist even when KaiC is always held in a highly phosphorylated state [15]. They thus concluded that the clock is driven by both a TTC and a PPC, and suggested that the interactions between the two oscillators may enhance the robustness of the clock [15].

The PPC has been characterized experimentally in considerable detail. It is known, for example, that KaiC forms a homo-hexamer [15], KaiA a dimer [15], and KaiB a dimer [5, 15] or a tetramer [17]. KaiC has two phosphorylation sites per protein monomer, which are phosphorylated and dephosphorylated in a definite sequence as a result of KaiC's autokinase and autophosphatase activity [7, 8]. KaiA stimulates KaiC phosphorylation [20, 21], while KaiB negates the effect of KaiA [20–23]. Thanks to the wealth of available experimental data, the PPC has proven an unusually fruitful system for mathematical modeling [1, 7, 16, 24–26, 28–31].

The TTC appears to encompass several different regulatory pathways and is much less well understood. Multiple lines of evidence indicate that circadian promoter activity can be achieved without any specific *cis*-regulatory element [33–35], suggesting that the clock may regulate transcription at least in part through changes in chromosome compaction and superhelicity [34, 36, 37]. Several proteins important for transcriptional regulation of the *kaiBC* operon have also been identified. In particular, LabA and the sensor histidine kinase CikA have been implicated in negative feedback of phosphorylated KaiC on its own transcription during the subjective night [11, 13, 14, 38, 39], while the SasA histidine kinase, acting through the RpaA response regulator, seems to mediate positive feedback during the subjective day [40, 41]. Epistasis analysis suggests that LabA may likewise act through RpaA [38]. The picture that emerges is thus that during the phosphorylation phase of the PPC, KaiC activates *kaiBC* expression, while in the dephosphorylation phase, it represses *kaiBC* expression [39] (Fig. 1).

In this study, we perform stochastic simulations to investigate the roles of the PPC and the TTC. We first examine a situation in which the total number of each Kai protein is *constant*—they are neither produced nor destroyed—and only the PPC is operative. We show that in this case the PPC is highly robust against noise arising from the intrinsic stochasticity of chemical reactions. Even for reaction volumes smaller than the typical volume of a cyanobacterium, the correlation time is longer than that observed experimentally [9]. Living cells, however, constantly grow and divide, and proteins must thus be synthesized to balance dilution. In fact, dilution can be thought of as introducing an effective protein degradation rate set by the cell doubling time. We therefore next study a PPC in which the Kai proteins are produced and degraded with rates that are constant in time. The simulations reveal that protein synthesis and decay dramatically reduce the viability of the PPC; we predict that for a cell doubling time of 24 hours and a bacterial volume of 1 μm^3, the PPC dephases in roughly 10 days, much faster than real *S. elongatus* [9]. The same loss of oscillations is seen even in the limit of infinite volume, indicating it is not due solely to noise. Instead, the constant synthesis of proteins, which we assume are all initially created in the same phosphorylation state, necessarily in-
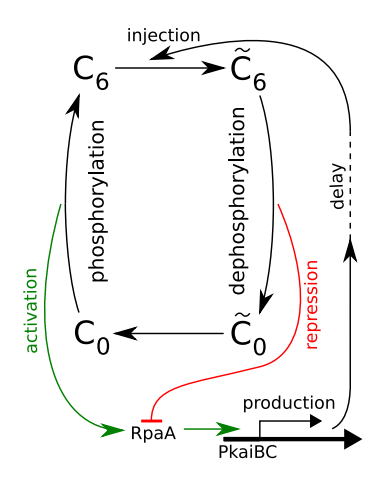

FIG. 1: A cartoon of how the TTC might interact with the PPC [39]. Active RpA activates *kaiBC* expression. During the phosphorylation phase, KaiC activates RpaA, while during the dephosphorylation phase, KaiC represses RpaA.

jects KaiC hexamers with the "wrong" phosphorylation levels at certain phases of the cycle [1, 42]; if these appear fast enough, they can destroy the oscillation. One role of the TTC is thus to introduce proteins only when the phosphorylation state of the freshly made KaiC matches that of the PPC. Our simulations of a combined PPC and TTC reveal that a TTC can indeed greatly enhance the robustness of the PPC, yielding correlation times consistent with those measured experimentally [9]. Finally, we consider whether the PPC is needed at all, or whether one could build an equally good circadian clock using only a TTC. We find that it is possible to construct a TTC with a period of 24 hours and the observed correlation time of a few months [9]. However, this comes at the expense of very high protein synthesis and decay rates, which impose an extra energetic burden on the cell. Our results thus suggest that a PPC allows for a more robust oscillator at a lower cost. Although our models are simplified, we argue in the Discussion section that our qualitative results are unavoidable consequences of the interaction between a circadian clock and cell growth and so should hold far more generally.

II. RESULTS

A. A protein phosphorylation cycle with constant protein concentrations is highly robust

In recent years, the PPC has been mathematically modelled with considerable success [1, 7, 16, 24–26, 28–31] (for a review, see [43]). All models endow KaiC with an intrinsic ability to cyclically phosphorylate and dephosphorylate itself, but they differ in how the cycles of the individual KaiC proteins are synchronized. In this manuscript, we adopt the model developed by us [1], which is one of several based on a mechanism that we

called "differential affinity" [1, 7, 24, 28]: KaiA stimulates KaiC phosphorylation, but the limited supply of KaiA dimers binds preferentially to those KaiC molecules that are falling behind in the cycle, allowing them to catch up. Specifically, in our model each KaiC hexamer can switch between an active conformational state C_i, where the number i of phosphorylated monomers tends to increase, and an inactive state $\widetilde{C}_i$, where i tends to decrease (Fig. 1); KaiA stimulates phosphorylation of active KaiC, but is sequestered by complexes containing KaiB and inactive KaiC. KaiC in the inactive state can thus delay the progress of fully dephosphorylated hexamers that have already switched back to the active state and are ready to be phosphorylated again. With A and B denoting, respectively, a KaiA dimer and a KaiB dimer, the model becomes:

$$C_i \overset{f_i}{\underset{b_i}{\rightleftarrows}} \widetilde{C}_i, \ C_i + A \overset{k_i^{\mathrm{Af}}}{\underset{k_i^{\mathrm{Ab}}}{\rightleftarrows}} AC_i \overset{k_{\mathrm{pf}}}{\rightarrow} C_{i+1} + A \quad (1)$$

$$\widetilde{C}_i + B \overset{2\tilde{k}_i^{\mathrm{Bf}}}{\underset{\tilde{k}_i^{\mathrm{Bb}}}{\rightleftarrows}} B\widetilde{C}_i, B\widetilde{C}_i + B \overset{\tilde{k}_i^{\mathrm{Bf}}}{\underset{2\tilde{k}_i^{\mathrm{Bb}}}{\rightleftarrows}} B_2\widetilde{C}_i \quad (2)$$

$$B_x\widetilde{C}_i + A \overset{x\tilde{k}_i^{\mathrm{Af}}}{\underset{\tilde{k}_i^{\mathrm{Ab}}}{\rightleftarrows}} AB_x\widetilde{C}_i, AB_2\widetilde{C}_i + A \overset{\tilde{k}_i^{\mathrm{Af}}}{\underset{2\tilde{k}_i^{\mathrm{Ab}}}{\rightleftarrows}} A_2B_2\widetilde{C}_i \quad (3)$$

$$C_i \overset{k_{\mathrm{ps}}}{\underset{k_{\mathrm{dps}}}{\rightleftarrows}} C_{i+1}, \widetilde{C}_i \overset{\tilde{k}_{\mathrm{ps}}}{\underset{\tilde{k}_{\mathrm{dps}}}{\rightleftarrows}} \widetilde{C}_{i+1} \quad (4)$$

$$B_x\widetilde{C}_i \overset{\tilde{k}_{\mathrm{ps}}}{\underset{\tilde{k}_{\mathrm{dps}}}{\rightleftarrows}} B_x\widetilde{C}_{i+1}, A_yB_x\widetilde{C}_i \overset{\tilde{k}_{\mathrm{ps}}}{\underset{\tilde{k}_{\mathrm{dps}}}{\rightleftarrows}} A_yB_x\widetilde{C}_{i+1} . \quad (5)$$

This model reproduces the phosphorylation behaviour of KaiC *in vitro* not only when all Kai proteins are present, but also when KaiA and/or KaiB are absent [1]. It moreover correctly predicted the experimentally observed disappearance of oscillations when the KaiA concentration is raised [6, 7], a success that strongly supports the idea that KaiA sequestration is the primary driver of synchronization. Our model does not feature monomer exchange between KaiC hexamers, an alternative means of synchronisation [25] that has been observed in experiments [5, 29]; we and others find that monomer exchange is not critical for stable oscillations [1, 7, 28]. In the *Supporting Information* (*SI*), we show that similar results are obtained with a model that focuses on the phosphorylation cycle of individual KaiC monomers [7, 8] rather than of KaiC hexamers and that includes a positive feedback loop.

We quantify our model's robustness to chemical noise by performing kinetic Monte Carlo simulations of the chemical master equation [4]. In our simulations, we vary the reaction volume, but keep the concentrations of the Kai proteins constant at levels comparable to those used in the *in vitro* experiments [5, 6]. Fig. 2A shows a time trace of the fraction $p(t)$ of phosphorylated KaiC monomers at a volume of order that of a cyanobacterium, while Fig. 2B gives, as a function of volume, the correlation number of cycles $n_{1/2}$, defined as the number of
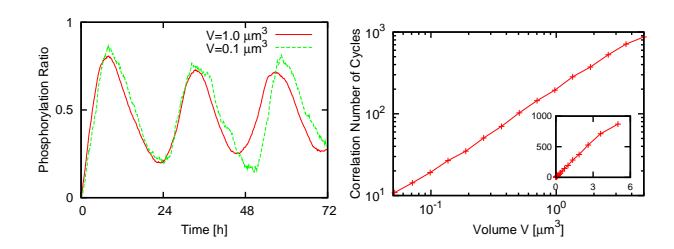

FIG. 2: The KaiC phosphorylation oscillator is highly stable when proteins are not synthesized or degraded. (A) Time trace of the phosphorylation ratio $p(t)$, *i.e.* the fraction of monomers that are phosphorylated, for volumes $V = 1\mu m^3$ and $V = 0.1\mu m^3$. (B) Correlation number of cycles, $n_{1/2}$, as a function of the volume. The protein concentrations are those used in the *in vitro* experiments [5, 6]: $[A]_T = 0.58\mu M; [B]_T = 1.75\mu M; [C]_T = 0.58\mu M$. For other parameters, see Table S1 of *SI*.

cycles after which the standard deviation in the phase of the oscillation is half a day [16]; in the *SI* we discuss our error estimates, which suggest that our computed $n_{1/2}$ values are typically accurate to within 15–20%. One issue that arises in comparing the simulation results to the measured *in vivo* clock robustness is that the Kai proteins appear to be present in living cells in a ratio at which the *in vitro* system would not oscillate. Kitayama *et al.* found that there are approximately 10,000 KaiC monomers but only 250–500 KaiA monomers per *S. elongatus* cell [22], corresponding to a roughly 6:1 KaiC hexamer to KaiA dimer ratio instead of the standard 1:1 ratio *in vitro* [5, 6]. It has been suggested that this discrepancy may indicate that the clock reactions are in fact confined to a subdomain of the whole cell from which some of the KaiB and KaiC molecules are excluded [22]; here, we adopt this hypothesis and assume that the Kai proteins are found in the physiologically relevant reaction volume in proportions comparable to those used in the *in vitro* experiments. If we take this volume to be $\sim 1\mu m^3$, comparable to the size of the entire cell, then Fig. 2B shows that $n_{1/2} \approx 200$, on the high side of the measured 166 ± 100 [9]. Even if we consider a volume of only $0.5\mu m^3$—small enough that the measured number of KaiA molecules is adequate to give the *in vitro* KaiA dimer concentration of $0.58\mu M$—we find that $n_{1/2} \approx 102$, still within the experimental bounds (in contrast to the predictions of some alternative models [7, 16]; see *SI*). Our model thus predicts that the PPC is very resistant to noise arising from the intrinsically stochastic nature of chemical reactions.

B. A phosphorylation cycle with constant protein synthesis and degradation rates is not stable

Fig. 2 shows that the phosphorylation cycle is highly robust when the total concentrations of the Kai proteins are strictly constant. But *in vivo* proteins are constantly being synthesized and degraded. To study how this af-
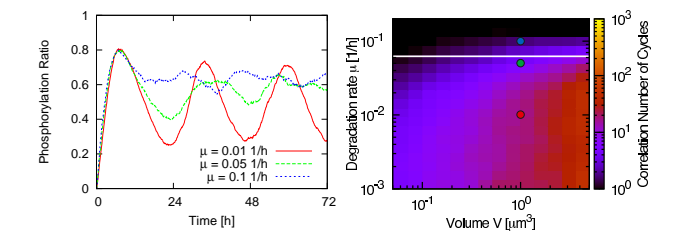
FIG. 3: A system in which the Kai proteins are produced and degraded with rates that are constant in time cannot sustain a stable phosphorylation cycle. (A) Time trace of the phosphorylation ratio $p(t)$ for three different degradation rates μ and $V = 1\mu\text{m}^3$. (B) Correlation number of cycles, $n_{1/2}$, as a function of the volume and degradation rate. The white line denotes the bifurcation line $\mu = 0.0621\text{h}^{-1}$, where the system undergoes a supercritical Hopf bifurcation in the deterministic limit; the three colored dots correspond to the three curves in panel A. All proteins are degraded with the same rate; KaiA, KaiB and KaiC are produced with rates such that the average total concentrations equal those used in the *in vitro* experiments (see Fig. 2).

fects the PPC, we consider a model in which the Kai proteins are produced and degraded in a stochastic (memoryless) fashion with rates that are constant in time, with the effects of active degradation [2] and of passive dilution lumped into a single first-order decay rate μ (see *SI*).

Fig. 3 shows the performance of the phosphorylation cycle as a function of degradation rate and cell volume; in all cases, the synthesis rates are adjusted so that the mean concentrations are constant and equal to those used in the previous section. The oscillator's robustness clearly decreases dramatically with increasing protein synthesis and decay rate. For a volume comparable to that of a cyanobacterium and a degradation rate of 0.03hr^{-1}, the correlation time is less than 20 days, much lower than that observed *in vivo* [9]. This degradation rate is precisely the effective rate arising from protein dilution with a cell doubling time of 24 hours. It is known, however, that KaiC is also degraded actively at a rate as high as 0.1hr^{-1} [2], leading to still worse stability.

The disappearance of the oscillations for higher protein synthesis and decay rates can be understood by noting that fresh KaiC hexamers are made in a fixed phosphorylation state, which then has to catch up with those of the proteins that are already in the cycle [1, 42]. When the degradation rate is high, the new proteins are likely to be degraded before the PPC can synchronise their phosphorylation levels; indeed, in the limit that the protein synthesis and decay rates go to infinity, $p(t)$ becomes constant in time and equal to the phosphorylation level of freshly made KaiC proteins. This is not a purely stochastic effect; the dashed bifurcation line of Fig. 3B shows that even in a deterministic model the oscillations disappear when the synthesis and decay rates become too big (see *SI*).

C. A protein phosphorylation cycle with a transcription-translation cycle is very stable

To sustain a phosphorylation cycle, KaiC has to be made in an oscillatory fashion: newly synthesized KaiC proteins have to be injected into the phosphorylation cycle at the moment that the phosphorylation states of the other proteins that are already in the cycle match the modification state of the fresh KaiC proteins [1]. This is the principal role of the transcription-translation cycle. Here, we present a model for how such a cycle might interact with the protein phosphorylation cycle (see Fig. 1). The model is inspired by that of Kondo *et al.* [39] and contains the following key ingredients:

1. RpaA activates kaiBC expression
Deletion of *rpaA* reduces the expression of clock-controlled genes, including that of *kaiBC* [38, 39, 41]. Since neither promoters nor transcription or chromosome-compaction factors have been identified that interact with RpaA [41], we make the phenomenological assumption that RpaA directly activates *kaiBC* expression [39].

2. RpaA is activated by KaiC when KaiC is in the active state
RpaA is activated via phosphorylation by the histidine kinase SasA, whose activity is in turn stimulated by KaiC [36, 41]; inactivation of SasA reduces *kaiBC* expression [38, 39, 41]. Moreover, SasA-RpaA phosphorylation occurs 4-8 hours before the peak of KaiC phosphorylation [41]. This suggests that partially phosphorylated KaiC that is on the active branch activates RpaA through SasA [39]. Since SasA phosphorylation, occurring on time scales of minutes [36], is much faster than KaiC phosphorylation, occurring on time scales of hours, we assume that the SasA dynamics can be integrated out.

3. RpaA is inactivated by KaiC when KaiC is in the inactive state
Inactivation of LabA [38] or CikA [39] increases *kaiBC* expression, with inactivation of both having a still stronger effect [39]. SasA inactivation can compensate for both LabA [38] and CikA inactivation [39], but RpaA inactvation cannot compensate for LabA inactivation [38]. Taken together, these results suggest that SasA, LabA, and CikA control *kaiBC* expression through different pathways, with at least the SasA and LabA pathways converging on RpaA [39]. Because phosphorylation of KaiC is critical for negative feedback on *kaiBC* expression [14], LabA and CikA appear to act downstream of phosphorylated KaiC [39]. Since the mechanisms by which LabA and/or CikA repress RpaA activation are unknown, we make the phenomenological assumption that KaiC on the inactive branch deactivates RpaA.

4. KaiC is injected into the system as fully phosphorylated hexamers
Imai *et al.* reported that newly synthesized KaiC is phosphorylated *in vivo* within 30 min [2], much faster than phosphorylation of KaiC hexamers *in vitro*, which

takes about 6 hours [7]; we thus assume that newly synthesized KaiC is injected into the system as fully phosphorylated KaiC hexamers.

5. KaiA and RpaA are synthesized at constant rates
The mRNA levels of *kaiA* and *rpaA* exhibit much weaker oscillations than those of *kaiB* and *kaiC* [33]. We therefore assume that *kaiA* and *rpaA* are expressed at constant rates.

6. The phosphorylation cycle in vivo is similar to that in vitro.

Fig. 1 shows a cartoon of this model, which is described by the reactions of Eqs. 1–5 for the PPC together with the following reactions for the TTC and the coupling between them:

$$\widetilde{R} + X \xrightarrow{k_a} R + X, \ \ R + \widetilde{X} \xrightarrow{k_i} \widetilde{R} + \widetilde{X} \tag{6}$$

$$\emptyset \underset{\tau;\sigma_\tau}{\overset{\beta_c[R]^4/(K^4+[R]^4)}{\Longrightarrow}} C_6 + 3B \tag{7}$$

$$\emptyset \xrightarrow{\beta_a} A, \ \ \emptyset \xrightarrow{\beta_r} \widetilde{R}, \tag{8}$$

$$R, \widetilde{R}, A, B, AC_i, B_x\widetilde{C}_i, A_yB_x\widetilde{C}_i \xrightarrow{\mu} \emptyset \tag{9}$$

Eq. 6 models activation of inactive RpaA, $\widetilde{R}$, by $X \in \{AC_2, \ldots AC_5\}$ and inactivation of active RpaA, R, by $\widetilde{X} \in \{A_yB_x\widetilde{C}_5 \ldots A_yB_x\widetilde{C}_2\}$. The model is robust to the precise choice of phosphoforms that activate and repress RpaA (see *SI*). Because KaiA enhances *kaiBC* expression [20], we assume that active KaiC bound to KaiA activates RpaA; a model in which both C_i and AC_i activate RpaA also generates oscillations, albeit less robustly (see *SI*). Eq. 7 models the activation of *kaiBC* expression by RpaA, using a Hill function with coefficient 4. We assume a normally distributed delay, denoted by the double arrow, with mean $\tau = 5$ hr and standard deviation $\sigma_\tau = 0.5$ hr, between the activation of *kaiBC* transcription and the appearance of KaiB and KaiC protein. The length of the delay is dictated by the requirement that new KaiC protein be produced when its phosphorylation state matches that of the PPC. Eq. 8 models constitutive expression of *kaiA* and *rpaA*. Eq. 9 describes degradation of all species with the same rate constant μ; we ignore rhythmic KaiC degradation [2], which is not essential to produce a robust clock. In the *SI* we discuss a more detailed model that includes cell growth and binomial partitioning upon cell division, which appreciably increases noise without changing qualitative trends. Although one can think of our model in loose terms as consisting of coupled transcriptional and post-translational oscillators, it cannot be mathematically decomposed into two separate oscillatory systems, each with its own variables, nor can the strength of the coupling between the two cycles be independently tuned. It is thus formally quite different from textbook models of coupled oscillators [10].

Fig. 4B shows the robustness of this PPC-TTC model as a function of cell volume and protein degradation rate μ; when μ is varied, all three protein synthesis rates β_α
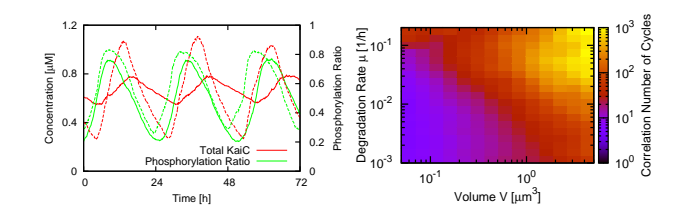

FIG. 4: The combination of a TTC and a PPC can generate stable circadian rhythms. (A) Time trace of the phosphorylation ratio $p(t)$ and total KaiC concentration $[C]_T$ for $V = 1\mu m^3$ and $\mu = 0.03 hr^{-1}$ (solid lines) and $0.1 hr^{-1}$ (dashed lines). (B) Correlation number of cycles, $n_{1/2}$, for $p(t)$ as a function of the volume and degradation rate μ. The protein synthesis rates are varied with the degradation rates such that the average protein concentrations equal those used *in vitro* (see Fig. 2).

are adjusted so that the average protein concentrations are unchanged and comparable to those of the models considered above. As expected, $n_{1/2}$ decreases with decreasing cell volume. Its dependence on the degradation rate, however, is markedly different from that seen with constant KaiC synthesis (Fig. 3B): A PPC sustained by a TTC becomes *more* robust with increasing decay rate. If we assume that proteins are lost only through dilution, then for a bacterial volume of $1\,\mu m^3$ and a cell doubling time of 24 hours (corresponding to a decay rate $\mu = 0.03 hr^{-1}$), the correlation time is about 200 days, consistent with the value measured experimentally [9]. If proteins are also degraded actively, increasing μ, this excellent behavior improves still further; even for $V = 0.5\mu m^3$, $n_{1/2} \approx 120$ for $\mu = 0.1 hr^{-1}$. This is in stark contrast to the stability of a PPC without a TTC, which we have seen is hardly stable for a protein lifetime of about 10 hours (Fig. 3B).

D. A protein phosphorylation cycle dramatically enhances the robustness of a transcription-translation cycle

Figs. 3B and 4B show that a TTC can greatly improve the robustness of a PPC. One might thus ask whether the PPC is needed at all, or whether an adequate clock can be built with only a TTC. To address this question, we modify the PPC-TTC model (Eqs. 6–9) so that it consists only of a TTC:

$$\emptyset \underset{\tau;\sigma_\tau}{\overset{\beta_c[R]^4/(K^4+[R]^4)}{\Longrightarrow}} C, \ \ \emptyset \xrightarrow{\beta_r} R, \ \ C, R \xrightarrow{\mu} \emptyset \tag{10}$$

$$\widetilde{R} \xrightarrow{k_a^t} R, \ \ C + R \xrightarrow{k_i^t} C + \widetilde{R} \tag{11}$$

In the simulations, we adjust the delay τ and the synthesis rate β for each choice of the degradation rate μ such that the oscillation period is 24 hours and the average KaiC concentration is comparable to that of the other models considered so far (see *SI*). We also investigated the simplest possible TTC model, namely one in which

KaiC directly represses its own synthesis; this gave very similar results (see *SI*).

Fig. 5B shows for a bacterial volume of approximately $1\,\mu m^3$ the robustness of this TTC-only model as a function of the degradation rate, together with the results for the PPC-TTC model (Fig. 4B) and for the PPC-only model with constant synthesis rates (Fig. 3B). The TTC-only model's behavior is the opposite of that of the PPC-only model; the TTC-only model is most stable for *high* degradation rates, and its robustness falls dramatically when μ drops below $0.2\mathrm{hr}^{-1}$. The combined TTC-PPC model, however, is robust for all degradation rates—its correlation time interpolates between those of the TTC-only model for large μ and of the PPC-only model for small μ. Importantly, the relative advantage of the combined model is greatest when $1/\mu$ is of order the oscillator period, and this is precisely the regime where physiological degradation and dilution rates for *S. elongatus* fall [2]. Further, the combined oscillator does much better than either oscillator alone; in contrast, when two conventional phase oscillators with comparable noise levels are coupled, one expects only about a factor of two gain in $n_{1/2}$ [10].

Dilution puts a lower bound on the degradation rate, which means that a stable oscillator cannot be based on a PPC only, especially when the growth rate of the bacterium is large. The degradation rate can, on the other hand, be increased by active degradation. For high degradation rates, *i.e.* $\mu > 0.2\mathrm{hr}^{-1}$, an oscillator based only on transcriptional feedback can be sufficiently robust (Fig. 5B). However, to balance these high decay rates, the protein synthesis rates have to be correspondingly large, which is energetically costly [47]. Combining a PPC with a TTC makes it possible to dramatically improve the robustness while keeping the protein synthesis rates the same. While a phosphorylation cycle does not come entirely for free [48], this suggests that a PPC combined with a TTC gives the best performance-to-cost ratio.

The question remains why a PPC so effectively enhances the robustness of a TTC. Fig. 5A shows, for the full PPC-TTC model, time traces of the concentration of RpaA, the sum of the concentrations of the KaiC phosphoforms that activate RpaA, and the sum of those that repress RpaA; for comparison, we also show the KaiC concentration in the TTC-only model. In the TTC-only model, the KaiC concentration varies slowly, and the concentration threshold for *kaiBC* repression is crossed at a shallow angle. In contrast, in the PPC-TTC model the concentration of active RpaA switches rapidly between a value that is well above the activation threshold for *kaiBC* expression and one that is well below it. Such sharp threshold crossings minimize the effect of fluctuations in the concentration of the regulatory protein on the timing of the switch between *kaiBC* activation and *kaiBC* repression. RpaA's abrupt switching is a direct consequence of the sharp rise and fall in the concentrations of the KaiC phosphoforms that regulate RpaA. This in turn
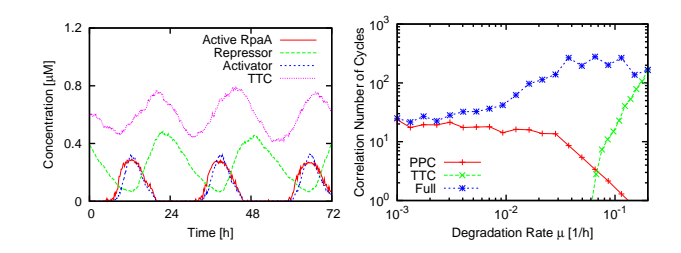

FIG. 5: A PPC in combination with a TTC generates robust rhythms over a wide range of degradation rates. (A) Time traces of the concentrations of active RpaA and of the KaiC phosphoforms that activate ("activator") and repress ("repressor") RpaA for the PPC-TTC model ($V = 1\mu m^3$ and $\mu = 0.03\mathrm{hr}^{-1}$), and KaiC for the TTC-only model ($V = 1\mu m^3$ and $\mu = 0.12\mathrm{hr}^{-1}$; for $\mu = 0.03\mathrm{hr}^{-1}$ the TTC does not oscillate); (B) Correlation number of cycles as a function of degradation rate μ for the PPC, TTC, and combined TTC-PPC model ($V = 1\mu m^3$); for the TTC, $n_{1/2}$ was computed for $[C](t)$ rather than for $p(t)$. The protein synthesis rates are varied with the degradation rates such that the average concentrations equal those used in the *in vitro* experiments (see Fig. 2).

stems not so much from the oscillation in the total concentration of KaiC, but from the phosphorylation cycle at the multiple phosphorylation sites of KaiC: The concentrations of the various phosphoforms approach zero in certain parts of the cycle (Fig. 5A), even though the total KaiC concentration remains relatively large throughout (Fig. 4A). Indeed, the stability of the circadian rhythm in the PPC-TTC model is mostly determined by the KaiC phosphorylation cycle, which, as Fig. 2B shows, is highly robust. It thus seems that the phosphorylation cycle is the principal pacemaker, even though a transcription-translation cycle is needed to sustain it and can, in fact, raise its robustness above the limiting value at zero protein synthesis and decay rate (Fig. 5B).

III. DISCUSSION

The evidence is accumulating that circadian rhythms are driven by both transcription-translation and protein-modification cycles not just in cyanobacteria but even in higher organisms [1, 49]. Our analysis suggests that both cycles are required to generate stable circadian rhythms in growing cells over a wide range of conditions. On the one hand, it is intrinsically difficult for a TTC to generate oscillations when the average protein decay time is long compared to the oscillation period. Indeed, the speed of protein degradation (and/or dilution) sets a simple upper bound on the size of any oscillation; if only a small fraction of the proteins can be degraded in one oscillation cycle, then any modulation of the total protein concentration must necessarily have a low amplitude and so be very susceptible to noise. In cells whose doubling time is of order tens of hours (comparable to the 24 hour clock period) or longer, a TTC alone can thus function robustly

only at the expense of high rates of protein synthesis and active protein degradation. On the other hand, a protein modification cycle must fail when protein turnover becomes faster than the clock period: Proteins are then typically degraded and replaced by new molecules in the wrong modification state before they can pass through the full cycle, destroying the oscillation. While a TTC is thus required to sustain a protein modification cycle at higher growth rates, a modification cycle can also greatly enhance the performance of a TTC, especially at lower protein synthesis and decay rates, where the modification cycle can be exploited to set the rhythm of gene expression. The protein phosphorylation cycle of KaiC is intrinsically very robust, because KaiC is present in relatively large copy numbers and because a KaiC hexamer must go through many individual phosphorylation and dephosphorylation steps in each oscillation period. These two characteristics together are responsible for the reliable and pronounced oscillations in the concentrations of the various phosphoforms of KaiC (Fig. 5A), which, in turn, drive the robust rhythm of *kaiBC* expression.

Our combined PPC-TTC model is consistent with a number of experimental observations. It not only matches the average oscillations of the phosphorylation level and the total KaiC concentration in wildtype cells (Fig. 4A), but also reproduces the observation that even in the presence of an excess of KaiA, the total KaiC concentration still oscillates with a circadian period [15] (see *SI*). Yet, because quite a few elements of the TTC have not been characterized experimentally, our model of the TTC is necessarily rather simplified and phenomenological; not surprisingly, some observations thus cannot be reproduced. For example, our model predicts that the phase of the oscillation in KaiC abundance lags behind that of the phosphorylation level by a few hours, while experiments seem to show that these oscillations are more in phase [7, 15]. This may be due to our simplifying assumption that KaiC is produced as fully phosphorylated hexamers. While phosphorylation of fresh KaiC has been reported to occur within 30 minutes [2], fragmentary evidence suggests that hexamerisation is slow [50]; one would then expect to detect KaiC monomers in experiments several hours before our simulations report the presence of fully functional hexamers. We believe, however, that while our model is simplified, it does capture the essence of a coupled TTC and PPC: that is, it is built around a protein that not only regulates its own synthesis, but also undergoes a protein modification cycle, where the different modification states either activate or repress protein synthesis. Moreover, the basic trends we observe can largely be explained by the arguments of the preceding paragraph, which depend only on the comparison of a protein decay timescale with the oscillation period; we thus expect that our qualitative results should apply to any system that exploits both a protein

modification cycle and a transcription-translation cycle to generate circadian rhythms.

In *S. elongatus*, the period of the circadian rhythm is insensitive to changes in the growth rate [51, 52]. Since protein synthesis and decay rates, on the other hand, tend to vary with the growth rate [53], the question arises whether the period of the oscillator as predicted by our model is robust to such variations. In the *SI* we show that a ten-fold increase in the synthesis and degradation rates of all proteins only decreases the period by 10-20%. The reason is that the period of the oscillator is mostly determined by the intrinsic period of the phosphorylation cycle (Fig. 5A). The latter does not depend on the absolute protein synthesis and decay rates, although it does depend on the ratio of the concentrations of the Kai proteins [1, 5, 6]. Clearly, it would be of interest to investigate how the ratio of the concentrations of the Kai proteins varies with the growh rate.

Finally, how could our predictions be tested experimentally? The most important testable prediction of our analysis is that the PPC requires a TTC when the growth rate is high. Kondo and coworkers have demonstrated that a PPC can function in the absence of a TTC [7]. These experiments were performed under constant dark (DD) conditions, which means that the growth rate was (vanishingly) small, protein synthesis was halted, and even protein decay was probably negligible, since the KaiC level was rather constant [7]. These experiments are consistent with our predictions, but the critical test would be to increase the growth rate while avoiding any circadian regulation of *kaiBC* expression. This means that the cyanobacteria must be grown under constant light (LL) conditions. Moreover, one would need to bring *kaiBC* expression under the control of a promoter that is constitutively active. However, most promoters of *S. elongatus* [33, 34], and even many heterologous promoters from *E. coli* [35], are influenced by the circadian clock. Nevertheless, a number of promoters have been reported that exhibit arhythmic activity [33], and these might be possible candidates. A still more challenging experiment would be to express the phosphorylation cycle in the bacterium *E. coli* [54]. Our analysis predicts that in growth-arrested cells, the phosphorylation cycle should be functional, while in normal growing *E. coli* cells, with cell doubling times of roughly 1 hour, the oscillations should cease to exist.

A. Acknowledgments

[1] Johnson CH, Egli M, Stewart PL (2008) Structural insights into a circadian oscillator. *Science* 322:697–701.

[2] Elowitz MB, Levine AJ, Siggia ED, Swain PS (2002) Stochastic gene expression in a single cell. *Science* 297:1183 – 1186.

[3] Liu C, Weaver DR, Strogatz SH, Reppert SM (1997) Cellular construction of a circadian clock: period determination in the suprachiasmatic nuclei. *Cell* 91:855–60.

[4] Yamaguchi S, et al. (2003) Synchronization of cellular clocks in the suprachiasmatic nucleus. *Science* 302:1408–12.

[5] Mihalcescu I, Hsing W, Leibler S (2004) Resilient circadian oscillator revealed in individual cyanobacteria. *Nature* 430:81–85.

[6] Amdaoud M, Vallade M, Weiss-Schaber C, Mihalcescu I (2007) Cyanobacterial clock, a stable phase oscillator with negligible intercellular coupling. *Proc Natl Acad Sci USA* 104:7051–6.

[7] Tomita J, Nakajima M, Kondo T, Iwasaki H (2005) No transcription-translation feedback in circadian rhythm of KaiC phosphorylation. *Science* 307:251–4.

[8] Nakajima M, et al. (2005) Reconstitution of circadian oscillation of cyanobacterial KaiC phosphorylation in vitro. *Science* 308:414–5.

[9] Kitayama Y, Nishiwaki T, Terauchi K, Kondo T (2008) Dual KaiC-based oscillations constitute the circadian system of cyanobacteria. *Genes Dev* 22:1513–21.

[10] Pikovsky A, Rosenblum M, Kurths J (2001) *Synchronization, a universal concept in nonlinear sciences* (Cambridge University Press).

[11] Ishiura M, et al. (1998) Expression of a gene cluster *kaiABC* as a circadian feedback process in cyanobacteria. *Science* 281:1519–23.

[12] Xu Y, Mori T, Johnson CH (2000) Circadian clock-protein expression in cyanobacteria: rhythms and phase setting. *EMBO J* 19:3349–57.

[13] Nakahira Y, et al. (2004) Global gene repression by KaiC as a master process of prokaryotic circadian system. *Proc Natl Acad Sci USA* 101:881–5.

[14] Nishiwaki T, et al. (2004) Role of KaiC phosphorylation in the circadian clock system of *Synechococcus elongatus* PCC 7942. *Proc Natl Acad Sci USA* 101:13927–32.

[15] Kageyama H, Kondo T, Iwasaki H (2003) Circadian formation of clock protein complexes by KaiA, KaiB, KaiC, and SasA in cyanobacteria. *J Biol Chem* 278:2388–95.

[16] Kageyama H, et al. (2006) Cyanobacterial circadian pacemaker: Kai protein complex dynamics in the KaiC phosphorylation cycle in vitro. *Mol Cell* 23:161–71.

[17] Hitomi K, Oyama T, Han S, Arvai AS, Getzoff ED (2005) Tetrameric architecture of the circadian clock protein KaiB. A novel interface for intermolecular interactions and its impact on the circadian rhythm. *J Biol Chem* 280:19127–35.

[18] Nishiwaki T, et al. (2007) A sequential program of dual phosphorylation of KaiC as a basis for circadian rhythm in cyanobacteria. *EMBO J* 26:4029–37.

[19] Rust MJ, Markson JS, Lane WS, Fisher DS, O'Shea EK (2007) Ordered phosphorylation governs oscillation of a three-protein circadian clock. *Science* 318:809–12.

[20] Iwasaki H, Nishiwaki T, Kitayama Y, Nakajima M, Kondo T (2002) KaiA-stimulated KaiC phosphorylation in circadian timing loops in cyanobacteria. *Proc Natl Acad Sci USA* 99:15788–93.

[21] Xu Y, Mori T, Johnson CH (2003) Cyanobacterial circadian clockwork: roles of KaiA, KaiB and the *kaiBC* promoter in regulating KaiC. *EMBO J* 22:2117–26.

[22] Kitayama Y, Iwasaki H, Nishiwaki T, Kondo T (2003) KaiB functions as an attenuator of KaiC phosphorylation in the cyanobacterial circadian clock system. *EMBO J* 22:2127–34.

[23] Williams SB, Vakonakis I, Golden SS, LiWang AC (2002) Structure and function from the circadian clock protein KaiA of *Synechococcus elongatus*: a potential clock input mechanism. *Proc Natl Acad Sci USA* 99:15357–62.

[24] Takigawa-Imamura H, Mochizuki A (2006) Predicting regulation of the phosphorylation cycle of KaiC clock protein using mathematical analysis. *J Biol Rhythms* 21:405–16.

[25] Emberly E, Wingreen NS (2006) Hourglass model for a protein-based circadian oscillator. *Phys Rev Lett* 96:038303.

[26] Mehra A, et al. (2006) Circadian rhythmicity by autocatalysis. *PLoS Comput Biol* 2:e96.

[27] van Zon JS, Lubensky DK, Altena PRH, ten Wolde PR (2007) An allosteric model of circadian KaiC phosphorylation. *Proc Natl Acad Sci USA* 104:7420–7425.

[28] Clodong S, et al. (2007) Functioning and robustness of a bacterial circadian clock. *Mol Syst Biol* 3:90.

[29] Mori T, et al. (2007) Elucidating the ticking of an in vitro circadian clockwork. *PLoS Biol* 5:e93.

[30] Miyoshi F, Nakayama Y, Kaizu K, Iwasaki H, Tomita M (2007) A mathematical model for the Kai-protein-based chemical oscillator and clock gene expression rhythms in cyanobacteria. *J Biol Rhythms* 22:69–80.

[31] Yoda M, Eguchi K, Terada TP, Sasai M (2007) Monomer-shuffling and allosteric transition in KaiC circadian oscillation. *PLoS One* 2:e408.

[32] Eguchi K, Yoda M, Terada TP, Sasai M (2008) Mechanism of robust circadian oscillation of KaiC phosphorylation in vitro. *Biophys J* 95:1773–84.

[33] Ito H, et al. (2009) Cyanobacterial daily life with Kai-based circadian and diurnal genome-wide transcriptional control in *Synechococcus elongatus*. *Proc Natl Acad Sci USA* 106:14168–73.

[34] Vijayan V, Zuzow R, O'Shea EK (2009) Oscillations in supercoiling drive circadian gene expression in cyanobacteria. *Proc Natl Acad Sci USA* 106:22564–8.

[35] Ditty JL, Williams SB, Golden SS (2003) A cyanobacterial circadian timing mechanism. *Annu Rev Genet* 37:513–43.

[36] Smith RM, Williams SB (2006) Circadian rhythms in gene transcription imparted by chromosome compaction in the cyanobacterium *Synechococcus elongatus*. *Proc Natl Acad Sci USA* 103:8564–9.

[37] Woelfle MA, Xu Y, Qin X, Johnson CH (2007) Circadian rhythms of superhelical status of DNA in cyanobacteria. *Proc Natl Acad Sci USA* 104:18819–24.

[38] Taniguchi Y, et al. (2007) *labA*: a novel gene required for negative feedback regulation of the cyanobacterial circadian clock protein KaiC. *Genes Dev* 21:60–70.

[39] Taniguchi Y, Takai N, Katayama M, Kondo T, Oyama T (2010) Three major output pathways from the KaiABC-

based oscillator cooperate to generate robust circadian *kaiBC* expression in cyanobacteria. *Proc Natl Acad Sci USA*.

[40] Iwasaki H, et al. (2000) A KaiC-interacting sensory histidine kinase, SasA, necessary to sustain robust circadian oscillation in cyanobacteria. *Cell* 101:223–33.

[41] Takai N, et al. (2006) A KaiC-associating SasA-RpaA two-component regulatory system as a major circadian timing mediator in cyanobacteria. *Proc Natl Acad Sci USA* 103:12109–14.

[42] Ito H, et al. (2007) Autonomous synchronization of the circadian KaiC phosphorylation rhythm. *Nat Struct Mol Biol* 14:1084–8.

[43] Markson JS, O'Shea EK (2009) The molecular clockwork of a protein-based circadian oscillator. *FEBS Lett* 583:3938–47.

[44] Nakajima M, Ito H, Kondo T (2010) In vitro regulation of circadian phosphorylation rhythm of cyanobacterial clock protein KaiC by KaiA and KaiB. *FEBS Lett* 584:898–902.

[45] Gillespie DT (1977) Exact stochastic simulation of coupled chemical reactions. *J. Phys. Chem.* 81:2340 – 2361.

[46] Imai K, Nishiwaki T, Kondo T, Iwasaki H (2004) Circadian rhythms in the synthesis and degradation of a master clock protein KaiC in cyanobacteria. *J Biol Chem* 279:36534–9.

[47] Dekel E, Alon U (2005) Optimality and evolutionary tuning of the expression level of a protein. *Nature* 436:588–592.

[48] Terauchi K, et al. (2007) ATPase activity of KaiC determines the basic timing for circadian clock of cyanobacteria. *Proc Natl Acad Sci USA* 104:16377–81.

[49] Merrow M, Roenneberg T (2007) Circadian clock: time for a phase shift of ideas? *Curr Biol* 17:R636–8.

[50] Mori T, et al. (2002) Circadian clock protein KaiC forms ATP-dependent hexameric rings and binds DNA. *Proc Natl Acad Sci USA* 99:17203–8.

[51] Mori T, Binder B, Johnson CH (1996) Circadian gating of cell division in cyanobacteria growing with average doubling times of less than 24 hours. *Proc Natl Acad Sci USA* 93:10183–8.

[52] Kondo T, et al. (1997) Circadian rhythms in rapidly dividing cyanobacteria. *Science* 275:224–7.

[53] Klumpp S, Zhang Z, Hwa T (2009) Growth rate-dependent global effects on gene expression in bacteria. *Cell* 139:1366–75.

[54] Tozaki H, Kobe T, Aihara K, Iwasaki H (2008) An attempt to reveal a role of a transcription/translation feedback loop in the cyanobacterial KaiC protein-based circadian system by using a semi-synthetic method. *Int J Bioinform Res Appl* 4:435–44.

Supporting Information

Robust circadian clocks from coupled protein modification and transcription-translation cycles

David Zwicker, David K. Lubensky and Pieter Rein ten Wolde

I.   THE MODEL

A.   Protein phosphorylation cycle

The model for the KaiC protein phosphorylation cycle (PPC) is described by reactions (1)-(5) of the main text, which we repeat here:

$$C_i \underset{b_i}{\overset{f_i}{\rightleftarrows}} \widetilde{C}_i, \qquad\qquad C_i + A \underset{k_i^{Ab}}{\overset{k_i^{Af}}{\rightleftarrows}} AC_i \overset{k_{pf}}{\rightarrow} C_{i+1} + A, \tag{S1}$$

$$\widetilde{C}_i + B \underset{\tilde{k}_i^{Bb}}{\overset{2\tilde{k}_i^{Bf}}{\rightleftarrows}} B\widetilde{C}_i, \qquad\qquad B\widetilde{C}_i + B \underset{2\tilde{k}_i^{Bb}}{\overset{\tilde{k}_i^{Bf}}{\rightleftarrows}} B_2\widetilde{C}_i, \tag{S2}$$

$$B_x\widetilde{C}_i + A \underset{\tilde{k}_i^{Ab}}{\overset{x\tilde{k}_i^{Af}}{\rightleftarrows}} AB_x\widetilde{C}_i, \qquad\qquad AB_2\widetilde{C}_i + A \underset{2\tilde{k}_i^{Ab}}{\overset{\tilde{k}_i^{Af}}{\rightleftarrows}} A_2B_2\widetilde{C}_i, \tag{S3}$$

$$C_i \underset{k_{dps}}{\overset{k_{ps}}{\rightleftarrows}} C_{i+1}, \qquad\qquad \widetilde{C}_i \underset{\tilde{k}_{dps}}{\overset{\tilde{k}_{ps}}{\rightleftarrows}} \widetilde{C}_{i+1}, \tag{S4}$$

$$B_x\widetilde{C}_i \underset{\tilde{k}_{dps}}{\overset{\tilde{k}_{ps}}{\rightleftarrows}} B_x\widetilde{C}_{i+1}, \qquad\qquad A_yB_x\widetilde{C}_i \underset{\tilde{k}_{dps}}{\overset{\tilde{k}_{ps}}{\rightleftarrows}} A_yB_x\widetilde{C}_{i+1} . \tag{S5}$$

Here, C_i denotes a KaiC hexamer in the active conformational state, in which the number i of phosphorylated monomers tends to increase, and $\widetilde{C}_i$ denotes a KaiC hexamer in the inactive conformational state in which i tends to decrease; A denotes a KaiA dimer, and B denotes a KaiB dimer. The reactions $C_i \rightleftarrows \widetilde{C}_i$ in Eq. S1 model the conformational transitions between active and inactive KaiC; the second set of reactions in Eq. S1 describe phosphorylation of active KaiC that is stimulated by KaiA; the reactions in Eqs. S2 and S3 model the sequestration of KaiA by inactive KaiC that is bound to KaiB; note that an inactive KaiC hexamer can bind up to two KaiA dimers; the reactions in Eqs. S4 and S5 model spontaneous phosphorylation and dephosphorylation of active and inactive KaiC. For a more detailed discussion of the model, we refer to [1].

B.   A PPC with constant protein synthesis and degradation rates

In the main text, we also discuss the performance of a model that includes not only a PPC, but also synthesis and degradation of the Kai proteins. These reactions are given by

$$\emptyset \overset{\beta_c}{\rightarrow} C_6 + 3B, \qquad\qquad \emptyset \overset{\beta_a}{\rightarrow} A, \tag{S6}$$

$$A, B, AC_i, B_x\widetilde{C}_i, A_yB_x\widetilde{C}_i \overset{\mu}{\rightarrow} \emptyset \tag{S7}$$

As explained in the main text, we assume that fresh KaiC is injected into the system as fully phosphorylated hexamers because phosphorylation of fresh KaiC proteins has been reported to be fast, *i.e.* occurring within 30 minutes [2]. However, the precise choice for the phosphoform of fresh KaiC is not so important in this model; it does not affect the robustness of this model. Because the KaiB and KaiC proteins are both products of the *kaiBC* operon, we choose to model the production of both proteins as a single reaction. We note that while in the model with the transcription-translation cycle, discussed in section I D, the delay in the synthesis reactions is critical, in the above model, where the Kai proteins are produced with rates that are constant in time, a delay would have no effect; the synthesis reactions are therefore modeled as simple, Poissonian birth reactions.

C. Deterministic PPC model with synthesis and degradation

To verify that the disappearance of oscillations as the degradation rate is increased is not a purely stochastic effect, we consider the model of Eqs. (S1)–(S7) in the deterministic limit of infinite volume and protein number. In this limit, the concentrations of the different proteins evolve according to deterministic rate equations. We make two further simplifying assumptions: First, we replace the two-step binding of KaiB to $\widetilde{C}_i$ with a trimolecular reaction that turns $\widetilde{C}_i$ directly into $B_2\widetilde{C}_i$, and making a similar change for binding of KaiA to the inactive branch. Second, we assume that binding and unbinding reactions are fast enough that they are effectively in steady state and thus explicitly keep track only of the concentrations of the various KaiC species; the concentrations of free KaiA and KaiB can then be inferred from conservation laws. The dynamical equations are then essentially the same as those given in Eqs. $44 - 47$ of our previous publication [1], with the addition of a linear decay term with rate μ for each species and of synthesis of C_6 with rate β_c:

$$\frac{d[C_i]_T}{dt} = \sigma_{i-1}^{ps}[C_{i-1}]_T + \sigma_{i+1}^{dps}[C_{i+1}]_T - (\sigma_i^{ps} + \sigma_i^{dps})[C_i]_T - \sigma_i^{Ff}[C_i]_T + \sigma_i^{Fb}[\widetilde{C}_i] \tag{S8}$$

$$+ \beta_c\delta_{i,6} - \mu[C_i]_T \tag{S9}$$

$$\frac{d[\widetilde{C}_i]}{dt} = \tilde{k}_{ps}[\widetilde{C}_{i-1}] + \tilde{k}_{dps}[\widetilde{C}_{i+1}] - (\tilde{k}_{ps} + \tilde{k}_{dps})[\widetilde{C}_i] + \sigma_i^{Ff}[C_i]_T - \sigma_i^{Fb}[\widetilde{C}_i]$$

$$- \tilde{\kappa}_i^{Bf}([B]_T - 2\sum_i[B_2\widetilde{C}_i]_T)^2[\widetilde{C}_i] + \frac{\tilde{\kappa}_i^{Bb}\widetilde{K}_i[B_2\widetilde{C}_i]_T}{\widetilde{K}_i + [A]^2} - \mu[\widetilde{C}_i] \tag{S10}$$

$$\frac{d[B_2\widetilde{C}_i]_T}{dt} = \tilde{k}_{ps}[B_2\widetilde{C}_{i-1}]_T + \tilde{k}_{dps}[B_2\widetilde{C}_{+1}]_T - (\tilde{k}_{ps} + \tilde{k}_{dps})[B_2\widetilde{C}_i]_T$$

$$+ \tilde{\kappa}_i^{Bf}([B]_T - 2\sum_i[B_2\widetilde{C}_i]_T)^2[\widetilde{C}_i] - \frac{\tilde{\kappa}_i^{Bb}\widetilde{K}_i[B_2\widetilde{C}_i]_T}{\widetilde{K}_i + [A]^2} - \mu[B_2\widetilde{C}_i]_T \ , \tag{S11}$$

where the concentration of free KaiA, $[A]$, is given by

$$[A] + \sum_{i=0}^N \frac{[A][C_i]_T}{K_i + [A]} + 2\sum_{i=0}^N \frac{[A]^2[B_2\widetilde{C}_i]_T}{\widetilde{K}_i^2 + [A]^2} - [A]_T = 0 \ . \tag{S12}$$

Here $[C_i]_T$ is the total concentration of KaiC hexamers with i phosphorylated monomers in the active state, whether or not complexed with KaiA, i.e $[C_i]_T = [C_i] + [AC_i]$; $[B_2\widetilde{C}_i]_T$ is defined similarly. The effective rate constants appearing in these equations depend on the concentration $[A]$ of free KaiA and are defined in terms of the more microscopic rate constants as follows: The effective (de)phosphorylation rates on the active branch are $\sigma_i^{ps} = (k_{ps}K_i + k_{pf}[A])/(K_i + [A])$ and $\sigma_i^{dps} = K_i k_{dps}/(K_i + [A])$. The effective flipping rates are given by $\sigma_i^{Ff} = f_i K_i/(K_i + [A])$ and $\sigma_i^{Fb} = b_i$, where f_i and b_i are the forward and backward flipping rates. The parameters $\tilde{\kappa}_i^{Bf}$ and $\tilde{\kappa}_i^{Bb}$ differ from $\tilde{k}_i^{Bf}$ and $\tilde{k}_i^{Bb}$, respectively, in that the κ's are rate constants for trimolecular reactions which are broken down into two successive bimolecular reactions in the stochastic simulations. The dissociation constants K_i satisfy $K_i = k_i^{Ab}/k_i^{Af}$; the $\widetilde{K}_i$ could be defined similarly in terms of forward and backward rates for KaiA binding to the inactive branch, but (just as with $\tilde{\kappa}_i^{Bf}$ and $\tilde{\kappa}_i^{Bb}$) these rates would differ from those used in the stochastic simulations, so we choose instead to quote the dissociation constants directly. Following [1], we choose values for the new parameters associated with trimolecular interactions such that time dependence of the phosphorylation ratio $p(t)$ matches the average behavior of the stochastic model.

To determine where oscillations disappear as μ is increased, we analyzed these equations using the XPPAUT implementation of the AUTO continuation package [3]. We found that, for the parameter values given in Table S1, the system undergoes a supercritical Hopf bifurcation at $\mu = 0.0621$ 1/h, as noted in the main text.

D. The PPC and TTC combined

The full model of the main text consists of a PPC, a transcription-translation cycle (TTC), and a pathway that couples these two cycles. This model is described by the reactions of Eqs. S1-S5 for the PPC, together with the

Constant Value

PPC (Eqs. 1-5 and S1-S5):

$k_{\mathrm{ps}}, \tilde{k}_{\mathrm{ps}}$	$0.025\ ^1/_{\mathrm{h}}$
$k_{\mathrm{dps}}, \tilde{k}_{\mathrm{dps}}$	$0.4\ ^1/_{\mathrm{h}}$
k_{pf}	$1.0\ ^1/_{\mathrm{h}}$
f_i	$\{10^{-6}, 10^{-5}, 10^{-4}, 10^{-3}, 10^{-2}, 10^{-1}, 10\}\ ^1/_{\mathrm{h}}$
b_i	$100\ ^1/_{\mathrm{h}}$
k_i^{Af}	$1.72 \cdot 10^{10}\ ^1/_{\mathrm{M \cdot h}}$
k_i^{Ab}	$\{1, 3, 9, 27, 81, 243, 729\}\ ^1/_{\mathrm{h}}$
$\tilde{k}_i^{\mathrm{Bf}}$	$1.72 \cdot 10^9 \times \{0.001, 0.1, 1, 1, 1, 1, 1\}\ ^1/_{\mathrm{M \cdot h}}$
$\tilde{k}_i^{\mathrm{Bb}}$	$\{10, 1, 1, 1, 1, 1, 1\}\ ^1/_{\mathrm{h}}$
$\tilde{k}_i^{\mathrm{Af}}$	$1.72 \cdot 10^9 \times \{0.01, 1000, 1000, 1000, 100, 0.001, 0.0001\}\ ^1/_{\mathrm{M \cdot h}}$
$\tilde{k}_i^{\mathrm{Ab}}$	$\{10, 1, 1, 1, 1, 1, 10\}\ ^1/_{\mathrm{h}}$

Deterministic PPC (Eqs. S8-S12):

$\tilde{\kappa}_i^{\mathrm{Bf}}$	$2.97 \cdot 10^{18} \times \{0.01, 1, 1, 1, 1, 1, 1\}\ ^1/_{\mathrm{M^2 \cdot h}}$
$\tilde{\kappa}_i^{\mathrm{Bb}}$	$100 \times \{10, 1, 1, 1, 1, 1, 1\}\ ^1/_{\mathrm{h}}$
K_i	$3.37 \cdot 10^{-25} \times \{\infty, 100, 1, 1, 100, \infty, \infty\}\ \mathrm{M^2}$

RpaA activation (Eqs. 6 + S13):

k_{a}	$8.6 \cdot 10^9\ ^1/_{\mathrm{M \cdot h}}$
k_{i}	$4.3 \cdot 10^9\ ^1/_{\mathrm{M \cdot h}}$

TTC (Eqs. 7-9, S14,S15):

K	$0.058\ \mu\mathrm{M}$
β_{a}	$\mu^{-1} \times 0.58\ \mu\mathrm{M}$
β_{r}	$\mu^{-1} \times 0.29\ \mu\mathrm{M}$
β_{c}	from optimization for $\langle[\mathrm{C}]\rangle = 0.58\ \mu\mathrm{M}$
τ	$5\,\mathrm{h}$
σ_τ	$0.5\,\mathrm{h}$

RpaA activation TTC-only (Eq. 11):

$k_{\mathrm{a}}^{\mathrm{t}}$	$1\ ^1/_{\mathrm{M \cdot h}}$
$k_{\mathrm{i}}^{\mathrm{t}}$	$100\ ^1/_{\mathrm{M \cdot h}}$

TABLE S1: The parameters used for the models of the main text. The degradation rate μ is a free parameter that we vary to explore different growth conditions. The numbers between the curly brackets in the right column correspond to the different KaiC phosphorylation states i in ascending order; values of ∞ for K_i indicate that a particular binding reaction is not allowed.

following reactions for the TTC and the coupling between them:

$$\widetilde{\mathrm{R}} + \mathrm{X} \xrightarrow{k_{\mathrm{a}}} \mathrm{R} + \mathrm{X}, \qquad\qquad \mathrm{R} + \widetilde{\mathrm{X}} \xrightarrow{k_{\mathrm{i}}} \widetilde{\mathrm{R}} + \widetilde{\mathrm{X}}, \tag{S13}$$

$$\emptyset \underset{\tau \pm \sigma_\tau}{\overset{\beta_{\mathrm{c}}[\mathrm{R}]^4/(K^4+[\mathrm{R}]^4)}{\Longrightarrow}} \mathrm{C}_6 + 3\mathrm{B}, \qquad\qquad \emptyset \xrightarrow{\beta_{\mathrm{a}}} \mathrm{A}, \qquad \emptyset \xrightarrow{\beta_{\mathrm{r}}} \widetilde{\mathrm{R}}, \tag{S14}$$

$$\mathrm{R}, \widetilde{\mathrm{R}}, \mathrm{A}, \mathrm{B}, \mathrm{AC}_i, \mathrm{B}_x\widetilde{\mathrm{C}}_i, \mathrm{A}_y\mathrm{B}_x\widetilde{\mathrm{C}}_i \xrightarrow{\mu} \emptyset. \tag{S15}$$

Here, R and $\widetilde{\mathrm{R}}$ denote the RpaA protein in its active and its inactive form, respectively. The X and $\widetilde{\mathrm{X}}$ in Eq. (S13) denote any of the phosphoforms of KaiC that mediate the activation and repression of RpaA, respectively; in the next section, we discuss the dependence of the results on precisely which phosphoforms are chosen. The double arrow indicates a reaction with a Gaussian distributed delay with mean τ and variance σ_τ. We thus assume that *kaiBC* expression is activated by RpaA, where the activity of RpaA is modulated by the PPC. In contrast, the expression of KaiA, KaiB, and RpaA is assumed to occur constitutively.

E. Parameters

Table S1 gives the values of the kinetic parameters used in the stochastic simulations based on the kinetic Monte Carlo algorithm developed by Gillespie [4]. Unless otherwise noted, we choose the total concentrations of the Kai proteins to match common conditions for the *in vitro* reaction system [5, 6]: $[\mathrm{A}]_{\mathrm{T}} = 0.58\,\mu\mathrm{M}$, $[\mathrm{B}]_{\mathrm{T}} = 1.75\,\mu\mathrm{M}$, and $[\mathrm{C}]_{\mathrm{T}} = 0.58\,\mu\mathrm{M}$.

Model	Activator	Repressor	Threshold K	$n_{1/2}$
a	AC_2, AC_3, AC_4, AC_5	$A_yB_x\widetilde{C}_2, \ldots, A_yB_x\widetilde{C}_5$	$0.058\,\mu M$	195
b	AC_3, AC_4	$A_yB_x\widetilde{C}_2, \ldots, A_yB_x\widetilde{C}_6$	$0.058\,\mu M$	118
c	AC_3, AC_4	$A_yB_x\widetilde{C}_3, \ldots, A_yB_x\widetilde{C}_4$	$0.058\,\mu M$	180
d	C_3, AC_3, C_4, AC_4	$A_yB_x\widetilde{C}_3, \ldots, A_yB_x\widetilde{C}_4$	$0.029\,\mu M$	39
e	$C_x, AC_x, \ x \in \{2,3,4,5\}$	$A_yB_x\widetilde{C}_3, \ldots, A_yB_x\widetilde{C}_4$	$0.029\,\mu M$	48

TABLE S2: Models with different output pathways from the PPC to the TTC. These models differ in the choice of phosphoforms that activate and repress RpaA, respectively. The maximal production rate β_c has been modified such that the average concentration of KaiC is $0.58\,\mu M$, as used in the *in vitro* experiments [5, 6]. In each case, $n_{1/2}$ is given for a volume $V = 1\,\mu m^3$ and a decay rate $\mu = 0.03\,h^{-1}$. Model "a" is the full model from the main text. To make the simulations tractable, we neglected repression of RpaA activation by KaiC phosphoforms that occur in negligible concentrations; consequently, the full list of phosphoforms that has the potential to repress RpaA is $\{B_2\widetilde{C}_6, B_2\widetilde{C}_5, AB_2\widetilde{C}_5, A_2B_2\widetilde{C}_5, B_2\widetilde{C}_4, AB_2\widetilde{C}_4, A_2B_2\widetilde{C}_4, B_2\widetilde{C}_3, AB_2\widetilde{C}_3, A_2B_2\widetilde{C}_3, B_2\widetilde{C}_2,$ $AB_2\widetilde{C}_2, A_2B_2\widetilde{C}_2\}$. Other parameters are given in Table S1.

II. RESULTS ARE INDEPENDENT OF DETAILS OF THE OUTPUT PATHWAY

In this section, we show that the precise choice of the KaiC phosphoforms that activate and repress RpaA is not critically important for the existence of oscillations. Table S2 shows the different models that we have considered, and Fig. S1 shows their time traces. It is seen that the time traces are very similar to those of the model in the main text, which is model "a" in Table S2. The most significant difference can be observed for the time trace of RpaA in models "d" and "e". In these models, not only C_xA activates RpaA, but also C_x, thus KaiC that is not bound to KaiA. The concentration of C_xA reaches zero during the dephosphorylation phase, and, as a result, the concentration of RpaA becomes zero during this phase in models "a"-"c". However, the concentration of C_x does not reach zero during the dephosphorylation phase, and consequently, there is some residual activation of RpaA during this phase in models "d" and "e". Nevertheless, RpaA activation during the dephosphorylation phase in these models does not manifest itself in the time traces of KaiC, because the concentration of active RpaA is still below the threshold for *kaiBC* expression. The oscillations of the phosphorylation level and total KaiC concentration are thus fairly similar in all models, although models "d" and "e" are less robust.
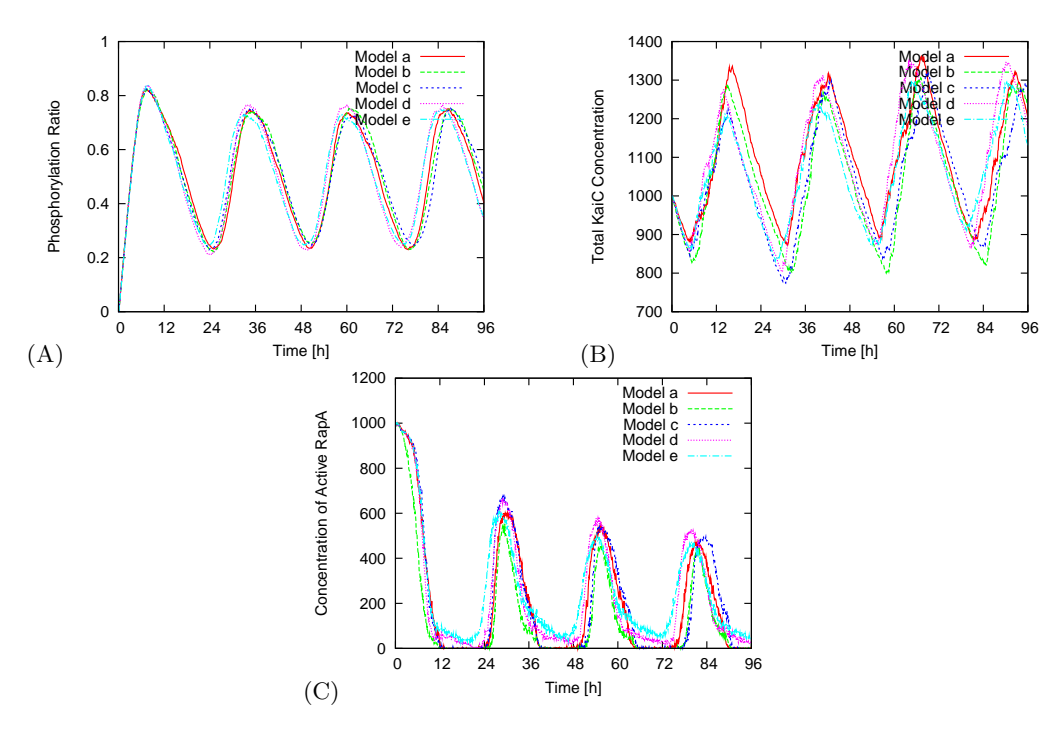

FIG. S1: Time traces of the stochastic simulations of models with different output pathways from the PPC to the TTC (see Table S2). The phosphorylation ratio (panel A) and the total concentration of KaiC (panel B) are fairly similar for all models studied.
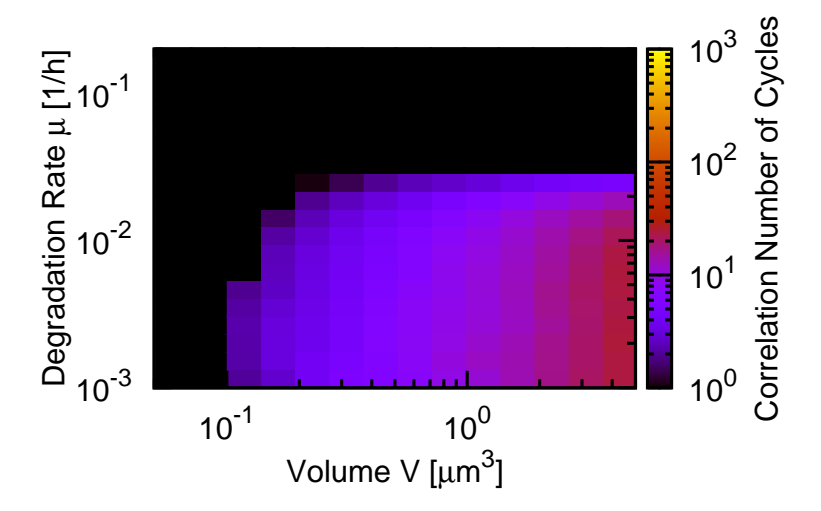
FIG. S2: Contour plot of the correlation number of cycles of the PPC model of Rust *et al.* [7] with production and degradation of Kai proteins with rates that are constant in time, as a function of the volume and the degradation rate.

III. AN ALTERNATIVE PPC MODEL

In the main text, we argue that the synergy between a transcription-translation cycle and a protein modification cycle is a generic feature of clocks that exploit both cycles. To support this claim, we have studied a model in which our model of the PPC is replaced by that of Rust *et al.* [7]. This model describes a phosphorylation cycle at the level of KaiC monomers, rather than KaiC hexamers as in our model. In the Rust model, each KaiC monomer cycles between an unphosphorylated state "U", a singly phosphorylated state "T" where KaiC is phosphorylated at threonine 432, a doubly phosphorylated state "ST" where KaiC is phosphorylated at threonine 432 and serine 431, and a singly phosphorylated state "S" where KaiC is phosphorylated at serine 431 [7, 8]. This cycle is described by the reactions

$$\text{U} \leftrightarrow \text{T}, \qquad\qquad \text{T} \leftrightarrow \text{ST}, \qquad\qquad \text{ST} \leftrightarrow \text{S}, \qquad\qquad \text{S} \leftrightarrow \text{U} \tag{S16}$$

with reaction rates given by Eq. 5 of the supplementary material of Rust *et al.* [7]. These rates depend on the concentration of free KaiA, which is sequestered by KaiC in the S-state. We model KaiA sequestration explicitly:

$$\text{S} + \text{A} \leftrightarrow \text{AS}, \qquad\qquad\qquad \text{AS} + \text{A} \leftrightarrow \text{A}_2\text{S}. \tag{S17}$$

We picture sequestration to be fast and we picked a forward rate of $0.58\,1/_{\mu\text{M·s}}$ and a backward rate of $1/_{\text{s}}$ for both equations above. Dephosphorylation of KaiC in the S-state might occur even when KaiA is bound, in which case the KaiA protein is released from the complex. We define the output signal as

$$p(t) = \frac{[\text{T}] + [\text{ST}] + [\text{S}] + [\text{AS}] + [\text{A}_2\text{S}]}{[\text{U}] + [\text{T}] + [\text{ST}] + [\text{S}] + [\text{AS}] + [\text{A}_2\text{S}]}, \tag{S18}$$

which resembles the phosphorylation ratio in the case where we cannot distinguish between singly and doubly phosphorylated KaiC. The denominator in the above expression is also the total KaiC monomer concentration. We use the same concentrations as Rust *et al.*, [KaiA] = $1.3\,\mu$M (active KaiA monomers) and [KaiC] = $3.4\,\mu$M (KaiC monomers), and simulate this model using the Gillespie algorithm [4].

When we simulate this model for a volume $V = 1\,\mu\text{m}^3$, we find a period of $L = 21.4\,$h and a decay constant for the autocorrelation function of $\tau_d = 128\,$h. The corresponding correlation number of cycles is $n_{1/2} = 30$, which is lower than that observed experimentally, $n_{1/2} = 166 \pm 100$ [9], and lower than that of the PPC developed by us [1], for which $n_{1/2} \approx 200$. This is because the model of Rust *et al.* features a phosphorylation cycle at the level of KaiC monomers rather than KaiC hexamers as in our model. The concomitant reduction in the total number of phosphorylation steps in the cycle reduces the robustness in the model of Rust *et al.* [7].

A. The Rust model with constant protein synthesis and degradation

To study the behavior of the model of Rust *et al.* [7] under conditions in which cells grow and divide, we have to include protein degradation and make up for this by protein synthesis. As in the main text, when we vary the protein
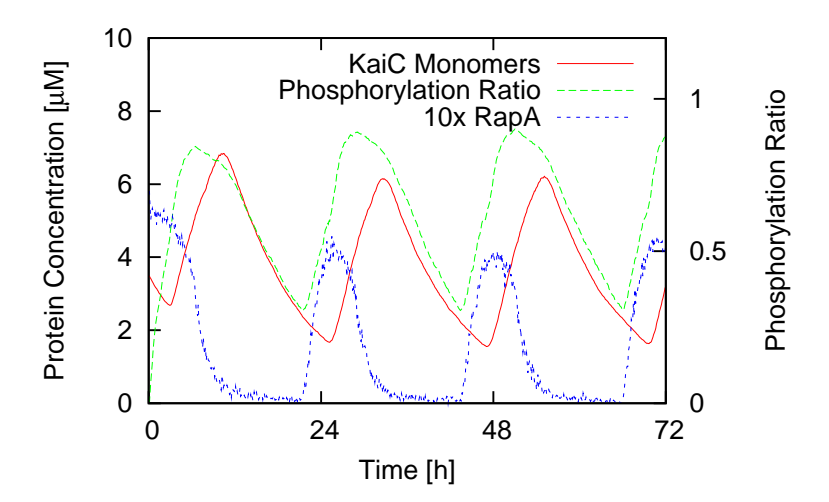
FIG. S3: Time trace of the Rust model [7] extended to include a TTC for $V = 1 \, \mu\text{m}^3$. Both the total concentration of KaiC and the phosphorylation level of KaiC show stable oscillations. The messenger protein RpaA concentration is shown tenfold and crosses the threshold of $K = 0.174 \, \mu\text{M}$ (≈ 100 molecules) reliably.

degradation rates, we adjust the protein synthesis rates such that the average protein concentrations are unchanged and similar to those used in the *in vitro* experiments [5, 6].

Figure S2 shows the results for this model. They are qualitatively the same as those of Figure 3 of the main text: the robustness decreases with decreasing volume and increasing degradation rate. Hence, not only in our model but also in that of Rust *et al.* [7], protein degradation can cause the oscillations to disappear. This supports our claim that a protein modification oscillator cannot function on its own when the cell's growth rate is high enough.

B.   The Rust model with a TTC

We will now show that a TTC can resurrect the PPC of Rust *et al.* [7]. We model the TTC as:

$$\emptyset \xrightarrow[\tau,\sigma_\tau]{\beta_c [\text{R}]^4/(K^4+[\text{R}]^4)} \text{ST}, \qquad\qquad \emptyset \xrightarrow{\beta_a} \text{A}, \qquad\qquad \emptyset \xrightarrow{\beta_r} \widetilde{\text{R}}, \qquad\qquad \text{(S19)}$$

$$\widetilde{\text{R}} + \text{T} \xrightarrow{k_a} \text{R} + \text{T}, \qquad\qquad \text{R} + \text{A}_x\text{S} \xrightarrow{k_i} \widetilde{\text{R}} + \text{A}_x\text{S}, \qquad\qquad x \in \{0, 1, 2\}, \qquad\qquad \text{(S20)}$$

$$\text{A}, \text{R}, \widetilde{\text{R}}, \text{U}, \text{S}, \text{A}_x\text{S}, \text{T}, \text{ST} \xrightarrow{\mu} \emptyset. \qquad\qquad \text{(S21)}$$

where the first line describes the production of proteins to counteract their degradation and the second line summarizes the RpaA signaling pathway, where KaiC that is phosphorylated at the T site activates RpaA and KaiC that is phosphorylated at the S site represses RpaA activation. The parameters in this model are $\beta_c = 1.13 \, \mu\text{M/h}$, $K = 0.058 \, \mu\text{M}$, $\beta_a = 0.13 \, \mu\text{M/s}$, $\beta_r = 0.058 \, \mu\text{M/s}$, $k_a = k_i = 0.1 \, {}^1/_{\mu\text{M·s}}$, and the delay is $\tau = (3 \pm 0.3)$ h. Figure S3 shows the results of this model at a volume $V = 1 \, \mu\text{m}^3$. Analysing the autocorrelation function, we find a period $L = 22.5$ h and a correlation decay time of $\tau = 1832$ h leading to a correlation number of cycles of $n_{1/2} = 402$. Clearly, a TTC can also resurrect the PPC of Rust *et al.* [7], supporting our claim that the qualitative results of the main text should apply to any biological system that exploits both a protein modification cycle and a protein synthesis cycle to generate circadian rhythms.

IV.   THE EFFECT OF BURSTS

In the model of the main text, described in section I of this *SI*, we have concatenated transcription and translation into one gene-expression step. Moreover, we have ignored promoter-state fluctuations. Allowing for the explicit formation and translation of mRNA [10], as well as for slow promoter-state fluctuations [11, 12], could lead to bursts in protein synthesis, which are expected to lower the robustness of the TTC. This could potentially lower the stability of the clock. To address this, we have performed simulations of a model in which KaiB and KaiC are produced in bursts. We assume that 5 KaiC hexamers and 15 KaiB dimers are formed in each gene expression reaction (rather
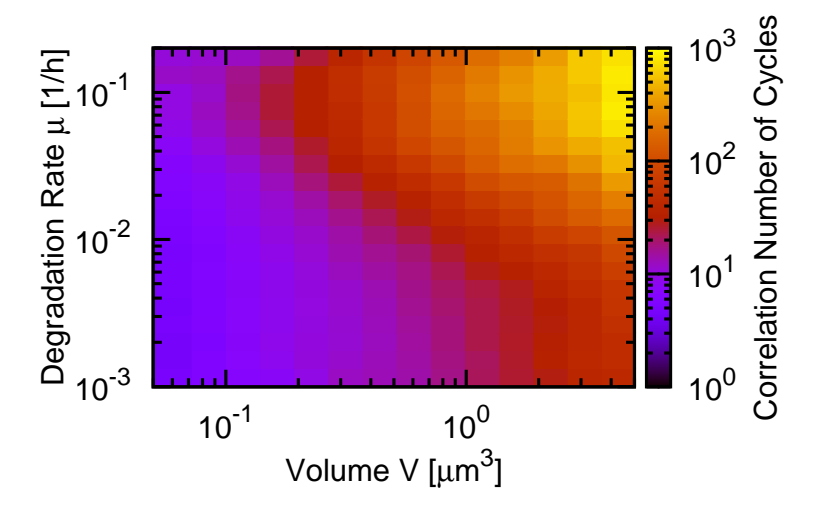
FIG. S4: The correlation number of cycles as a function of the degradation rate μ and the volume V for a TTC-PPC model that exhibits bursts in gene expression; upon a gene expression event, 5 KaiC molecules are produced and 15 KaiB dimers.

than the 1 and 3 of Eq. S14); this corresponds to typical burst sizes observed experimentally [10] in *E. coli*. Eq. S14 is thus replaced by:

$$\emptyset \underset{\tau \pm \sigma_\tau}{\overset{\beta_c [R]^4 / (K^4 + [R]^4)}{\Longrightarrow}} 5C_6 + 15B. \tag{S22}$$

Fig. S4 shows the resulting phase diagram. As expected, it is similar to Fig. 4 of the main text, which shows the results of the PPC-TTC model without bursts in gene expression. The robustness of the model with bursts is lower, but not very much so: $n_{1/2} = 150$ for the model with bursts versus $n_{1/2} = 195$ for the model without bursts shown in the main text ($\mu = 0.03 \text{hr}^{-1}$ and $V = 1\mu\text{m}^3$ in both cases). We believe that this relatively small reduction in the clock's stability is due to the stabilizing effect of the PPC.

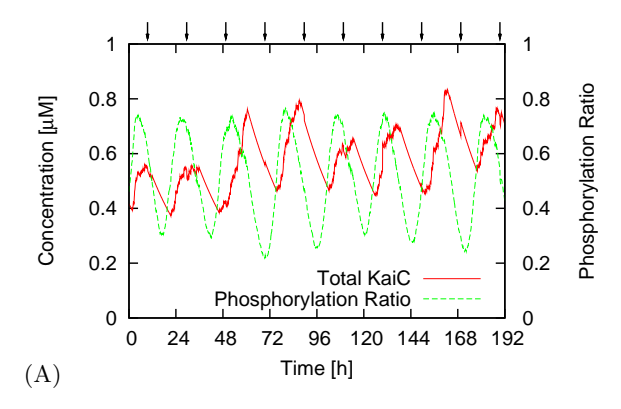## V. THE FULL MODEL WITH VOLUME GROWTH AND BINOMIAL PARTITIONING

Living cells constantly grow and divide, and proteins thus have to be synthesized to balance dilution. In the main text, we argued that the principal effect of dilution is to introduce an effective degradation rate set by the cell doubling time. Here, we show that this is indeed the case: we study a model in which growth, cell division and binomial partitioning of the proteins upon cell division are modeled explicitly [13], and show that its qualitative behavior is similar to the model of the main text, in which the volume is held constant and protein degradation occurs at a rate that is constant in time.

The model we consider here is the combined PPC-TTC model presented in the main text, but with the degradation reaction, Eq. 9, replaced by a scheme in which the bacterial volume V grows exponentially as

$$V(t) = V_0 e^{t\frac{\ln 2}{T_d}}, \tag{S23}$$

where T_d denotes the doubling time after which the volume reaches twice its minimum V_0 and cell division is triggered. Division includes dividing the volume by two, partitioning the proteins binomially [13], and deleting events on the queue of the delay associated with the KaiC production reaction with a probability of 0.5 for each daughter cell. To compare the results of this model with those from the main text, we take $T_d = \ln 2/\mu$, where μ is the protein degradation rate of the model in the main text; if proteins were to decay only by dilution in a cell with a doubling time T_d, then μ would be the effective protein degradation rate; if proteins are also degraded actively, then $\mu = \ln 2/T_d$ is a lower bound on the actual degradation rate.

Fig. S5 shows time traces of the total KaiC concentration and the KaiC phosphorylation level for this refined model. It is seen that the oscillations of the total KaiC concentration are more noisy than those in the model in which the Kai proteins are produced and degraded with rates that are constant in time (Fig. 4A of the main text). Clearly, binomial partitioning is a major source of noise, with the random removal of items from the queue associated with the KaiC synthesis reaction being the largest source of noise. Nonetheless, the oscillations of the KaiC phosphorylation level
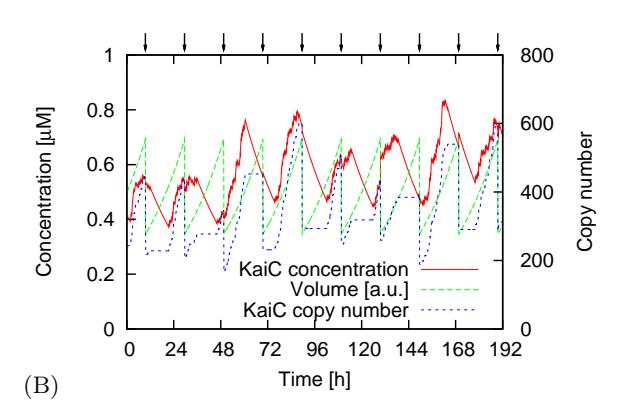
FIG. S5: Time traces of the full model, given by Eqs. 1-9 of the main text, modified to take into account cell division and binomial partitioning. Here, the cell divides when the volume reaches $V_m = 1.38\,\mu\text{m}^3$, which occurs every 20 h, as indicated by the arrows above the graph; a cell doubling time of 20 h corresponds to an effective degradation rate of $\mu = 0.035\,^1/\text{h}$. The average volume is $V = 1\,\mu\text{m}^3$. (A) Time traces of the phosphorylation level and the total KaiC concentration. (B) Time traces of the total KaiC concentration, the KaiC copy number and the volume. Please note that the time trace of the total KaiC concentration is hardly affected when cell division happens to occur during the degradation phase, while it has a relatively large effect when cell division happens to occur during the KaiC production phase; this is because the removal of items from the queue associated with the KaiC synthesis reaction effectively lowers the synthesis rate; indeed this explains the change in slope in the KaiC concentration during the production phase.

are much less affected, with the correlation number of cycles being $n_{1/2} = 88$. Indeed, while this model combining a TTC with a PPC is fairly robust, an oscillator with exponential volume growth and binomial partitioning built upon a TTC alone, is not stable. This supports our statement in the main text that a PPC can strongly enhance the robustness of a TTC. In a future publication, we will systematically study the effect of bursts in gene expression and binomial partitioning.

VI. ALTERNATIVE TTC MODELS

We not only studied the TTC model discussed in the main text, but also the simplest possible TTC model, namely one in which KaiC directly represses its own synthesis (with a delay):

$$\emptyset \; \underset{\tau;\sigma_\tau}{\overset{\beta K^4/(K^4+[\text{C}]^4)}{\Longrightarrow}} \; \text{C}, \; \text{C} \xrightarrow{\mu} \; \emptyset. \tag{S24}$$

The result of this model is shown in Fig. S6. It is seen that this TTC model behaves very similarly to that of the main text (compare Fig. 5B): it shows robust oscillations only for high degradation rates. Also including enzyme-mediated, zero-order protein degradation [14] does not qualitatively change this behavior. This supports our argument that the TTC has an intrinsic difficulty in generating oscillations when the doubling time is long and there is no strong active degradation.

In the simulations of Fig. 5B of the main text and Fig. S6 of the *SI* we vary the protein synthesis rate β_c and the protein-production delay τ such that the average KaiC concentration remains constant at the *in vitro* level [5, 6] and the period remains constant at 24 hours. This procedure means that as the degradation rate is increased, not only the synthesis rate has to be increased, but also the delay. One may wonder what would happen if the delay were kept constant and only the synthesis rate was adjusted, such that only the period remains constant at 24 hours; the average KaiC concentration is thus allowed to change. To address this, we show in Fig. S7 the results of a deterministic calculation based on the mean-field, chemical rate equations. Panel A shows as a function of the protein degradation rate μ, the KaiC synthesis rate β that keeps the oscillation period at 24 hours, for different values of the delay. It is seen that if the delay would be kept constant at 5-6 hours, as in the full model, the synthesis rate would have to be increased dramatically when the degradation rate is increased, to keep the period at 24 hours. This would raise not only the average KaiC concentration, but, more importantly, also the protein synthesis *rate*; this would increase the energetic cost of sustaining a TTC dramatically, as shown in Fig. S7B. In the main text, we keep not only the clock period constant, but also the average KaiC concentration. This means that when the degradation rate is increased, not only the synthesis rate, but also the delay is increased; however, even in this scenario, the cost of synthesizing proteins still increases markedly (Fig. S7B).
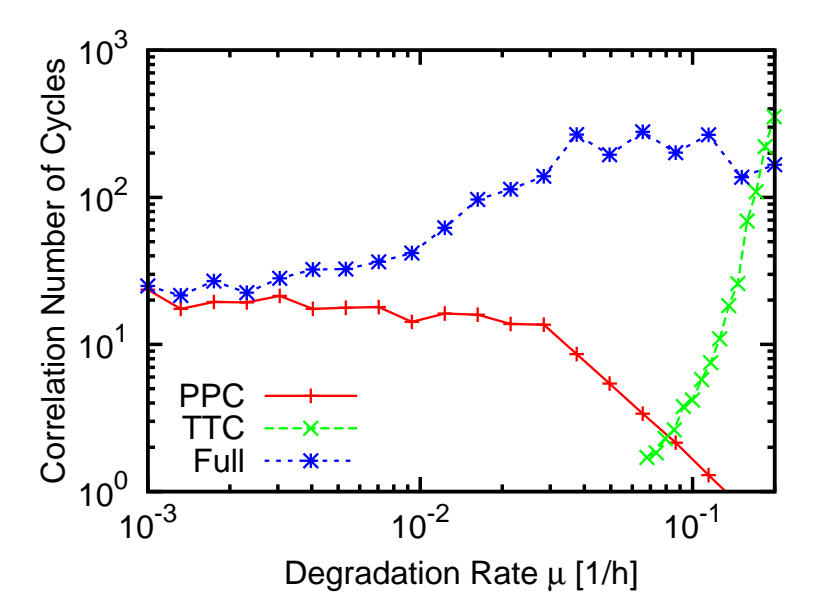
FIG. S6: A comparison of the performance of the PPC-only model (Eqs. S1 - S7), the full model including both PPC and TTC (Eqs. S1 - S5 and Eqs. S13 - S15), and the simplest possible TTC model, namely one in which KaiC directly represses its own synthesis (see Eq. S24). Compare to Fig. 5B of the main text.

VII. PERIOD AS A FUNCTION OF CELL VOLUME AND PROTEIN DEGRADATION RATE

Fig. S8 shows the period of the oscillation of the KaiC phosphorylation level in the full model of the main text (Eqs. 1–9) as a function of the cell volume and the protein degradation rate. As before, the protein synthesis rates are adjusted such that the average protein concentrations are constant and similar to those used in the *in vitro* experiments [5, 6]. It is seen that the dependence of the oscillation period on the cell volume and protein degradation rate is rather weak. This is because the rhythm of the clock is dictated by the PPC, which is insensitive to the absolute rates of
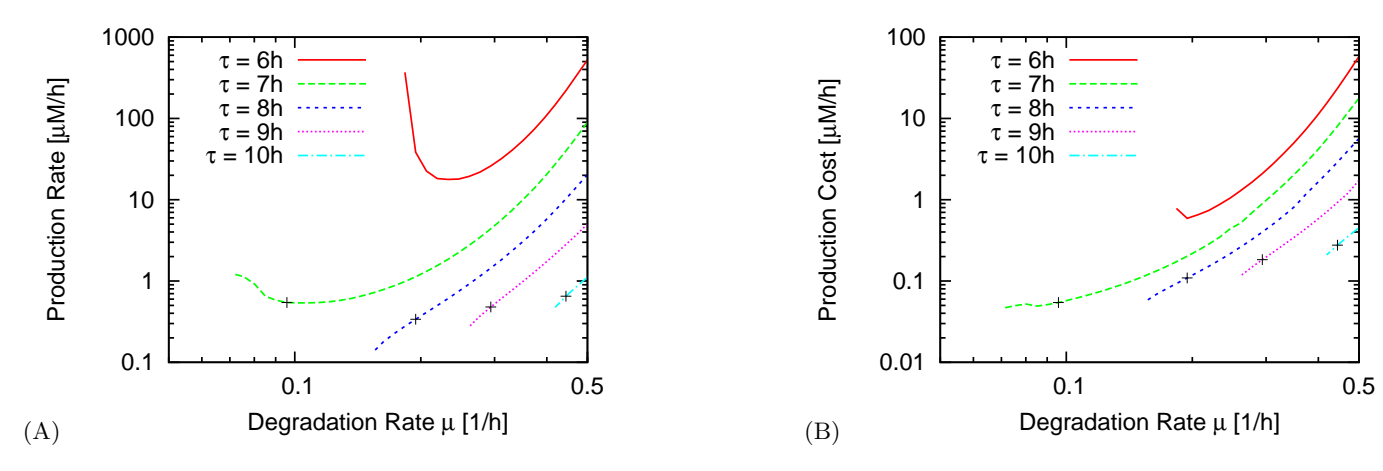

(A)

(B)

FIG. S7: The effect of changing the delay and the protein synthesis rate in a simple TTC based on Eq. S24. (A) The KaiC production rate β that keeps the oscillation period at 24 hours, as a function of the KaiC degradation rate, for different values of the delay τ. (B) The average synthesis rate (*i.e.* the average number of KaiC molecules produced per clock period), which is a measure for the cost associated with protein production during one period, as a function of the degradation rate. The model is a simple TTC in which KaiC directly represses its own synthesis, given by Eq. S24. The calculations were performed using the deterministic, mean-field chemical rate equations, because performing stochastic simulations with high production rates is prohibitively expensive. The crosses denote the points where not only the oscillation period is 24 hours, but also the average KaiC concentration equals that used in the main text, which is the KaiC concentration used in the *in vitro* experiments [5, 6]. The lines end for low degradation rates because the oscillations cease to exist. Panel A shows that to keep the clock period at 24 hours, the synthesis rate has to increase with the degradation rate, if the delay is kept constant. This not only raises the average KaiC concentration, but also increases the energetic cost of sustaining the TTC, as shown in panel B.
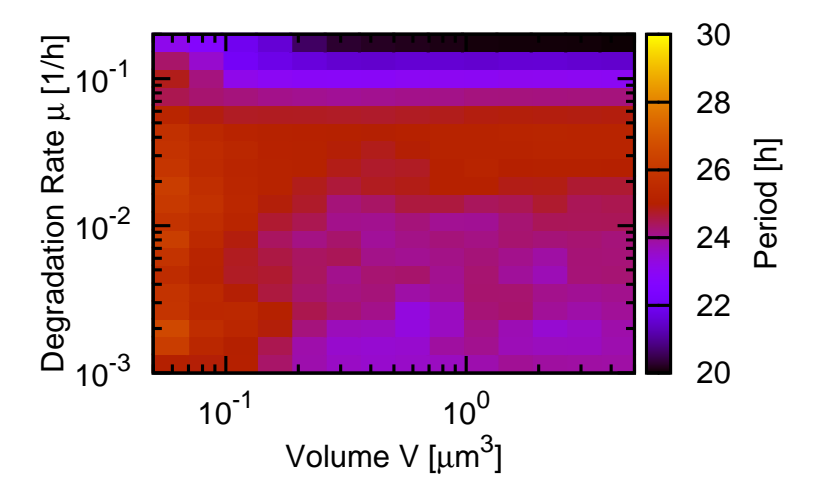
FIG. S8: Period of the oscillation in the KaiC phosphorylation level in the full model of the main text as a function of cell volume and protein degradation rate. When the degradation rate is varied, the protein synthesis rates are adjusted such that the average protein concentrations are constant and similar to those used in the *in vitro* experiments [5, 6]. The period is essentially independent of the volume, and exhibits only a weak dependence on the degradation rate μ.

protein synthesis and decay. We note here that the period of the oscillation, as well as its amplitude, would change if the *ratio* of the concentrations of the Kai proteins were changed. While the dependence of both the amplitude and the period of the *in vitro* PPC on the ratio of the concentrations of the Kai proteins has been characterized in detail [5, 6], the dependence of the *in vivo* oscillator on their ratio has not been studied experimentally.

VIII.   RHYTHMS OF *KAIBC* EXPRESSION WHEN *KAIA* IS OVEREXPRESSED
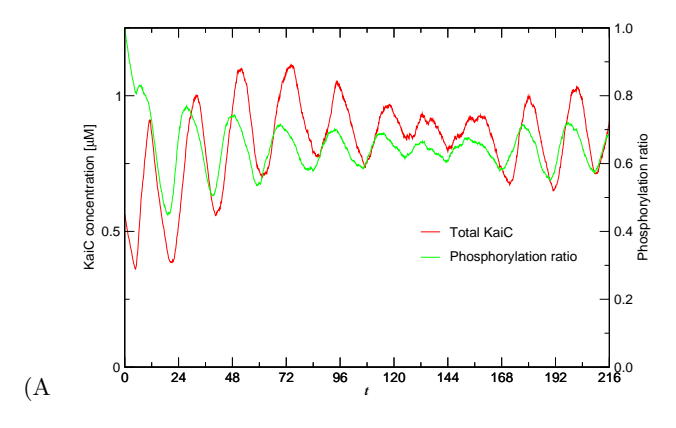
Kitayama *et al.* have shown that *kaiBC* expression oscillates with a circadian period in the presence of an excess of KaiA, although it is not clear whether these oscillations are sustained or damped [15]. Our PPC-TTC model of the main text, which is described by Eqs. S1—S5 and Eqs. S13—S15 above, generates oscillations in *kaiBC* expression with a period of 24 hours when *kaiA* is overexpressed threefold, as shown in Fig. S9A. This figure shows that the phosphorylation level also exhibits weak oscillations, which are not seen experimentally; this is due to the fact that our PPC model neglects phosphorylation of inactive KaiC, which is known to occur at high KaiA concentrations [7]. To rectify this, we have extended our model to include KaiA-stimulated phosphorylation of inactive KaiC, using the same reactions as those used for active KaiC; specifically, we add to the reactions of Eqs. S1—S5 and Eqs. S13—S15 the following reactions:

$$A_y B_x \widetilde{C}_i + A \underset{\tilde{k}_i^{Ab}}{\overset{\tilde{k}_i^{Af}}{\rightleftarrows}} A_y B_x \widetilde{C}_i A \overset{\tilde{k}_{pf}}{\rightarrow} A_y B_x \widetilde{C}_{i+1} + A, \tag{S25}$$

for each phosphorylation level i; the rate constants equal those of the corresponding reactions of active KaiC, except that the KaiA-KaiC association rate is reduced by a factor 100. All other rate constants are as in Table S1. We also include auto-activation of RpaA via

$$\widetilde{R} \overset{k_a^m}{\rightarrow} R, \tag{S26}$$

with $k_a^m = 25 \text{hr}^{-1}$. Auto-activation of RpaA becomes necessary because the concentrations of the KaiC phosphoforms that activate RpaA become very low when KaiA is in excess. (The freshly injected KaiC hexamers don't make it to the bottom of the phosphorylation cycle because of the excess KaiA.) This model not only matches the *in vitro* observation that, when an excess of KaiA is added during the dephosphorylation phase, the phosphorylation level of KaiC rises immediately [7], but also reproduces the *in vivo* oscillations of the total amount of KaiC when KaiA is overexpressed [15], as shown in Fig. S9B.
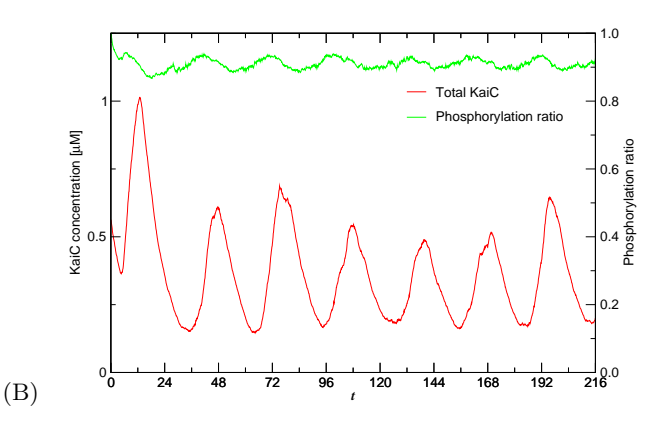
FIG. S9: The PPC-TTC model predicts oscillations in *kaiBC* expression when *kaiA* is overexpressed. (A) The original PPC-TTC model of Eqs. S1—S5 and Eqs. S13—S15 (B) The modified PPC-TTC model, given by the original model of Eqs. S1—S5 and Eqs. S13—S15 but extended to include KaiA-stimulated phosphorylation of inactive KaiC (Eq. S25) and auto-activation of RpaA (Eq. S26). Note that the total amount of KaiC exhibits pronounced, albeit somewhat arhythmic, oscillations, while the phosphorylation level is high and fairly constant. For both panels, the protein degradation rate is $\mu = 0.1\mathrm{hr}^{-1}$ and the volume is $V = 2.97\mu\mathrm{m}^3$; *kaiA* is overexpressed by a factor of 3.

IX. MEASURING THE ROBUSTNESS

In this section, we discuss how we calculate the correlation number of cycles $n_{1/2}$ for our various models. We begin with some theoretical background: Consider a phase variable $\varphi(t)$ that increases with an average frequency ω and is also subject to noise. Its time evolution can be written as

$$\frac{d\varphi(t)}{dt} = \omega + \xi(t) \qquad \text{with} \qquad \langle\xi(t)\xi(t')\rangle = \sigma^2\delta(t - t') . \tag{S27}$$

Here $\xi(t)$ is Gaussian white noise of strength σ^2, and $\langle\circ\rangle$ indicates averaging over different realizations of the noise. Integrating the equation with the initial condition $\varphi(0) = 0$ yields

$$\varphi(t) = \omega t + \mathcal{W}(t) , \tag{S28}$$

where $\mathcal{W}(t)$ is a Gaussian random variable with mean zero and variance

$$\left\langle (\varphi(t) - \omega t)^2 \right\rangle = \sigma^2 t. \tag{S29}$$

From this, we can construct an oscillating signal

$$x(t) = x_0 + a \cdot \sin\varphi(t) \tag{S30}$$

with mean x_0 and amplitude a. The autocorrelation function of (S30) is then

$$C(t') = \frac{\langle\delta x(t)\delta x(t + t')\rangle}{\langle\delta x(t)^2\rangle} = e^{-\frac{1}{4}\sigma^2|t'|} \cdot \cos(\omega t') , \tag{S31}$$

where $\delta x(t) \equiv x(t) - x_0$ is the deviation of the signal from its average value x_0. We thus expect that the correlation function is a sinusoid modulated by a single exponential decay.

A. Incorporating Amplitude Noise

Because the phase is the only "soft" direction of the dynamical system, one generically expects any noisy oscillator at long times to act similarly to the simple model of a phase oscillator just described. Nonetheless, a more realistic description would also include a fluctuating amplitude. We incorporate this behavior phenomenologically by including a time dependence in the amplitude:

$$a \rightarrow a(t) = a_0 + \xi_{(a)}(t) \qquad \Rightarrow \qquad x(t) = x_0 + \left(a_0 + \xi_{(a)}(t)\right) \cdot \sin\left(\omega t + \mathcal{W}(t)\right) \tag{S32}$$

where $\xi^{(a)(t)}$ denotes a Gaussian white noise process of strength σ_a^2 and therefore neglects correlations in the amplitude fluctuations. We can again calculate the correlation function analytically. By definition, we have $C(0) = 1$ for $t = 0$, but because $a(t)$ now contains a white noise term, $C(t)$ jumps discontinuously to a smaller value for any $t > 0$. One finds

$$C(t') = \frac{\langle \delta x(t) \delta x(t+t') \rangle}{\langle \delta x(t)^2 \rangle} = \underbrace{\frac{a_0^2}{a_0^2 + \sigma_a^2}}_{=\nu} e^{-\frac{1}{4}\sigma^2 |t'|} \cdot \cos(\omega t'), \qquad\qquad t' > 0. \qquad (S33)$$

Considering the more natural case of a finite correlation time in the amplitude noise, the picture will only change slightly: instead of jumping from 1 to ν at $\tau = 0$, the envelope will undergo a smooth transition for this envelope involving two time scales: a short time scale of order the correlation time of the amplitude fluctuations and a much longer time scale associated with the phase diffusion. In practice, we found that including amplitude fluctuations did not significantly change our estimate for $n_{1/2}$.

B. Computing the Correlation Number of Cycles

To calculate the correlation number of cycles $n_{1/2}$, we begin by using our simulation results to estimate the correlation function $C(t)$. After an initial equilibration phase of $500\,\mathrm{hr}$, we do simulations for $50{,}000\,\mathrm{hr}$. From these, we extract $N = 500{,}000$ values x_i for the time trace $x(t)$ at equidistant points in time, which we can then use to calculate the correlation function at times separated by an interval $\Delta t = 0.1\,\mathrm{h}$:

$$x_i = x(t_0 + i \cdot \Delta t), \qquad\qquad C(i \cdot \Delta t) = \frac{1}{(N-i) \cdot \langle \delta x^2 \rangle} \sum_{j=0}^{N-i} \delta x_j \delta x_{j+i} . \qquad (S34)$$

Here $x(t)$ is either the phosphorylation level $p(t)$ or the total concentration of KaiC hexamers. $p(t)$ is used for all cases except for models where there is only a TTC and a phosphorylation level cannot be defined.

Once $C(t)$ has been computed, it can be fitted to the form (S33) to determine the free parameters ν, σ^2, and ω. In practice we perform the fit using `gnuplot`, which in turn implements a Marquardt-Levenberg algorithm.

Finally, it remains to translate the fitted parameter values into an estimate of $n_{1/2}$. Eguchi $et\ al.$ define $n_{1/2}$ as the number of cycles after which the standard deviation of the phase is π [16]. Thus, we have

$$\sqrt{\langle [\varphi(L \cdot n_{1/2}) - \omega t]^2 \rangle} = \pi \qquad\qquad \Rightarrow \qquad\qquad n_{1/2} = \frac{\pi^2}{L\sigma^2}, \qquad (S35)$$

where $L = 2\pi/\omega$ denotes the period and we have used Eq. (S29) to solve the left equation for $n_{1/2}$. The value of $n_{1/2}$ is then obtained by substituting the fitted values for σ^2 and ω. Using this method we can reliably measure $n_{1/2}$ from 1 to 1,000. The upper bound is given by fact that we only compute the correlation function $C(t)$ up to $t = 3{,}000\,\mathrm{h}$ and therefore correlation functions which decay on much longer timescales are difficult to detect.

Concerning the error bar on the computed $n_{1/2}$, it should be noted that there are two distinct sources of error: one due to statistical fluctuations, and one due to systematic errors, $e.g.$ that the correlation function cannot be fitted to Eq. S33. To estimate the former, for certain parameter values we repeated the procedure described above 32 times, $i.e.$ we performed 32 independent simulations and computed the mean and the standard deviation of the set of 32 independently estimated values for $n_{1/2}$. For $V = 1\mu\mathrm{m}^3$ and $\mu = 0.025\mathrm{hr}^{-1}$, this gave $n_{1/2} = 168 \pm 31$ (mean $\pm$ std. deviation) for the combined PPC-TTC model. To address the second type of error, we also computed $n_{1/2}$ using two different methods. One is the method of Eguchi $et\ al.$, which is based on examining the times at which the oscillation reaches its maximum in each cycle, and thus does not assume any particular form like Eq. (S30) for the oscillating signal [16]. The other method involves computing the width of the dominant peak in the power spectrum of the time traces. The three methods gave similar error bars and values for $n_{1/2}$ that agree within the error bar. While all methods gave the same result, we found the method based on the correlation function (Eq. S33) more robust for noisy oscillations at low cell volumes.

[1] van Zon JS, Lubensky DK, Altena PRH, ten Wolde PR (2007) An allosteric model of circadian KaiC phosphorylation. $Proc\ Natl\ Acad\ Sci\ USA$ 104:7420–7425.

[2] Imai K, Nishiwaki T, Kondo T, Iwasaki H (2004) Circadian rhythms in the synthesis and degradation of a master clock protein KaiC in cyanobacteria. *J Biol Chem* 279:36534–9.

[3] Ermentrout B (2002) *Simulating, Analyzing, and Animating Dynamical Systems: A Guide to Xppaut for Researchers and Students* (SIAM, Philadelphia).

[4] Gillespie DT (1977) Exact stochastic simulation of coupled chemical reactions. *J. Phys. Chem.* 81:2340 – 2361.

[5] Kageyama H, et al. (2006) Cyanobacterial circadian pacemaker: Kai protein complex dynamics in the KaiC phosphorylation cycle in vitro. *Mol Cell* 23:161–71.

[6] Nakajima M, Ito H, Kondo T (2010) In vitro regulation of circadian phosphorylation rhythm of cyanobacterial clock protein KaiC by KaiA and KaiB. *FEBS Lett.*

[7] Rust MJ, Markson JS, Lane WS, Fisher DS, O'Shea EK (2007) Ordered phosphorylation governs oscillation of a three-protein circadian clock. *Science* 318:809–12.

[8] Nishiwaki T, et al. (2007) A sequential program of dual phosphorylation of KaiC as a basis for circadian rhythm in cyanobacteria. *EMBO J* 26:4029–37.

[9] Mihalcescu I, Hsing W, Leibler S (2004) Resilient circadian oscillator revealed in individual cyanobacteria. *Nature* 430:81–85.

[10] Ozbudak EM, Thattai M, Kurtser I, Grossman AD, van Oudenaarden A (2002) Regulation of noise in the expression of a single gene. *Nat Gen* 31:69 – 73.

[11] Golding I, Paulsson J, Zawilski SM, Cox EC (2005) Real-time kinetics of gene activity in individual bacteria. *Cell* 123:1025–1030.

[12] van Zon JS, Morelli M, Tănase-Nicola, Ten Wolde PR (2006) Diffusion of transcription factors can drastically enhance the noise in gene expression. *Biophys J* 91:4350–4367.

[13] Swain PS, Elowitz MB, Siggia ED (2002) Intrinsic and extrinsic contributions to stochasticity in gene expression. *Proc. Natl. Acad. Sci. USA* 99:12795 – 12800.

[14] Mather W, Bennett MR, Hasty J, Tsimring LS (2009) Delay-induced degrade-and-fire oscillations in small genetic circuits. *Phys Rev Lett* 102:068105.

[15] Kitayama Y, Nishiwaki T, Terauchi K, Kondo T (2008) Dual KaiC-based oscillations constitute the circadian system of cyanobacteria. *Genes Dev* 22:1513–21.

[16] Eguchi K, Yoda M, Terada TP, Sasai M (2008) Mechanism of robust circadian oscillation of KaiC phosphorylation in vitro. *Biophys J* 95:1773–84.